Sedimentary Facies Analysis of the Third Eocene Member of Shahejie Formation in the Bonan Sag of Bohai Bay Basin (China): Implications for Facies Heterogeneities in Sandstone Reservoirs

Nadir Fawad [1,2], Taixun Liu [1,3,*], Daidu Fan [2] and Qazi Adnan Ahmad [4]

1   School of Geoscience, China University of Petroleum (East China), Qingdao 266555, China
2   State Key Laboratory of Marine Geology, Tongji University, Shanghai 200092, China
3   Function Laboratory of Marine Geo-Resource Evaluation and Exploration Technology,
    Qingdao National Laboratory for Marine Science and Technology, Qingdao 266071, China
4   Department of Earth System Sciences, Yonsei University 50 Yonsei-ro, Seodaemun-gu, Seoul 120749, Korea
*   Correspondence: taixunliu@gmail.com or liutx@upc.edu.cn

Abstract: The middle sub-member (Es3z) within the third member (Es3) of the Eocene Shahejie formation is the main source of the generation and accumulation of hydrocarbons in the lacustrine deltas of Bonan depression. Exploration and research work in different blocks is carried out separately. Types of sedimentary facies, and their vertical and lateral evolution in Es3z are not studied in detail. To fill this knowledge gap, we did a detailed analysis of facies and lithological characteristics through integrative studies of cores, well logs and seismic data. Identification of sedimentary structures and lithology of the reservoir zone from cores are calibrated with high-quality well logs and seismic data. Depositional facies in Es3z reservoirs are identified through analysis of sedimentary structures, grain size, log's trends and seismic sections. Es3z was deposited in the fan delta front setting where five facies associations are found, among them distributary channels consisting of MCS, CSg, PCSs, MS, RCL, WCS, PBSs, RCS and GBS lithofacies, natural levee containing DFs, and furthermore, sheet sand are associated to CBS and SSM lithofacies. GM, GGM and DGM lithofacies are related to inter-distributary deposits, whereas mouth bars consist of PLS, CS and CFS. Depositional history, flow direction of the sediments, and facies distribution are investigated through detailed facies mapping and cross-section profiling to show that the sediments were sourced from southeast to northwest. We found thicker succession of sedimentary profiles towards north and north-west directions. Belt distributary channel deposits, covering a wide range of areas, act as potential reservoirs along with mouth bar deposits, while mudstones in interdistributary channels act as a good source and seal rocks. The methodology adopted has great potential to explore the reservoirs of fan delta front in lacustrine deltas.

Keywords: sedimentary facies; Bohai Bay Basin; well logs; seismic sedimentary evolution

1. Introduction

The Bohai Bay Basin is located in the eastern part of China [1]. The basin is extended by 2600 km in length and 1200 km in width, with a total area of about 200,000 km^2 [1]. Researchers and experts, from both industry and academia, have been probing the Bohai Basin geologically, but intense studies are still needed to investigate unexplored hydrocarbons.

Currently, the good quality reservoirs in the Paleogene strata of the Bohai Basin make it one of the promising potential areas for future petroleum exploration and development. Although structural geology, geochemical characteristics, petroleum system, reservoir modeling, and sedimentary characteristics have been well studied in the Eocene Shahejie Formation [2–7], no integrated study has been conducted to understand depositional facies

models and reservoir architectures of the middle sub-member (Es3z) within the third member (Es3) of the Eocene Shahejie Formation.

Sandstone groups in the Es3z member are defined as a single depositional facies in the previous research works, and lithological characteristics and depositional facies associations are not studied in detail, and it is considered as a single stratigraphic unit [5–8]. Moreover, some facies interpretations might be debatable due to limited data. A lack of systematic studies in the targeted zone causes difficulties in finding new exploration wells. The prevailing challenge in the petroleum exploration and development is to identify sedimentary features of sandstone units thoroughly and achieve elaborate facies interpretations [9]. As reservoir heterogeneity is strongly related to the sedimentary facies changes that ultimately has an impact on finding new exploration goals.

For future exploration targets in reservoir zones, appropriate sedimentological study is needed to better understand the potential of future reservoirs as the pre-drilling process relies on geoscience techniques for evaluating sub-surface geology to probe the good quality reservoir rocks. For pursuing our work, high-resolution borehole logs are helpful to provide continuous digital records of the reservoir units, integrating with cores and seismic data to describe lithology, sedimentary textures, directions of paleo-flow, and sedimentary sequences. Depositional systems are well understood by calibrating cores with well logs and seismic data, and small-scale reservoir heterogeneity is characterized by high resolution open hole logs. These studies will be helpful to investigate the unexplored hydrocarbon resources.

The aim of the current study is to interpret lithological associations, sedimentary structures, and detail depositional facies associations in the Es3z sandstone groups. These studies mark a diagnostic criterion to determine lithofacies, keen observation of sedimentary structures through cores, lithology and facies distribution in the study area. These integrated studies help us to predict the sedimentology of the reservoir and give us a better understanding of the reservoir characterization. Although the aforementioned methods have importance, some uncertainties may exist within the information extracted due to the lack of outcrops in the study area. This issue can be overcome by continuous core logging, and high-quality seismic data. The results obtained are a calibration of high-quality open hole well logs, core samples and 3D seismic data.

For a better understanding of the reservoir intervals, we analyzed, divided and investigated the facies associations of five sandstone groups that were investigated one by one. Facies of the fan deltaic system are recognized in the Es3z sandstones group in the Bonan Sag of Bohai Bay Basin, deposited in fan delta front settings. Five facies associations were identified in five sandstone groups that are sourced from south-east to north and north-west. Hence, our study could aid the exploration of future prospects in Es3z sandstone bodies. It will also enhance our understanding of the 3D depositional model that enables us to pursue simulation studies to recover remaining oil and to find new exploration targets in the all-sandstone units.

2. Geological Settings

The Bohai Bay Basin is located in the eastern part of the north China craton [10]. It is a Mesozoic and Cenozoic sedimentary basin, bounded by the Tan-Lu Fault Zone on its eastern side and the Taihang Mountain east fault zone to the west [11]. Right-lateral strike-slip and extensional faults have contributed to form the current shape of the basin [12,13]. Sixty-five fault depressions are found above the basement, which are mainly controlled by four sets of faults striking towards NNE, NE, NW and WNW [14]. The Bohai Bay Basin is segmented by the Cangxian and Chengning uplifts and others into several depressions, namely Hebei, Linqing, Huanghua, Jiyang, Liaodong Bay and Liaohe depressions [14]. In the Neogene period, the basin got tectonic stability and the fault activity decreased, while slow rifting in the basin is still experienced [15].

Bonan Sag

Bonan sag is considered as an extensional tectonic unit, developed in an extensional regime having both gentle and steep slope belts on south and north flanks, respectively (Figure 1) [3,16]. It is located in the mid-west of the Jiyang depression, and connected with the Chengdong uplift to the north through the Chengnan–Chengdong fault, and via Gudao uplift to the east (Figure 1). To the south, the Bonan sag is connected with the Chenjiazhuang uplift, and the Yihezhuang uplift to the west (Figure 1). During the deposition of the Eocene Shahejie formation, many alluvial fans, and fan deltas were developed, showing faulted depression, rigorous subsidence and quick deposition [15].
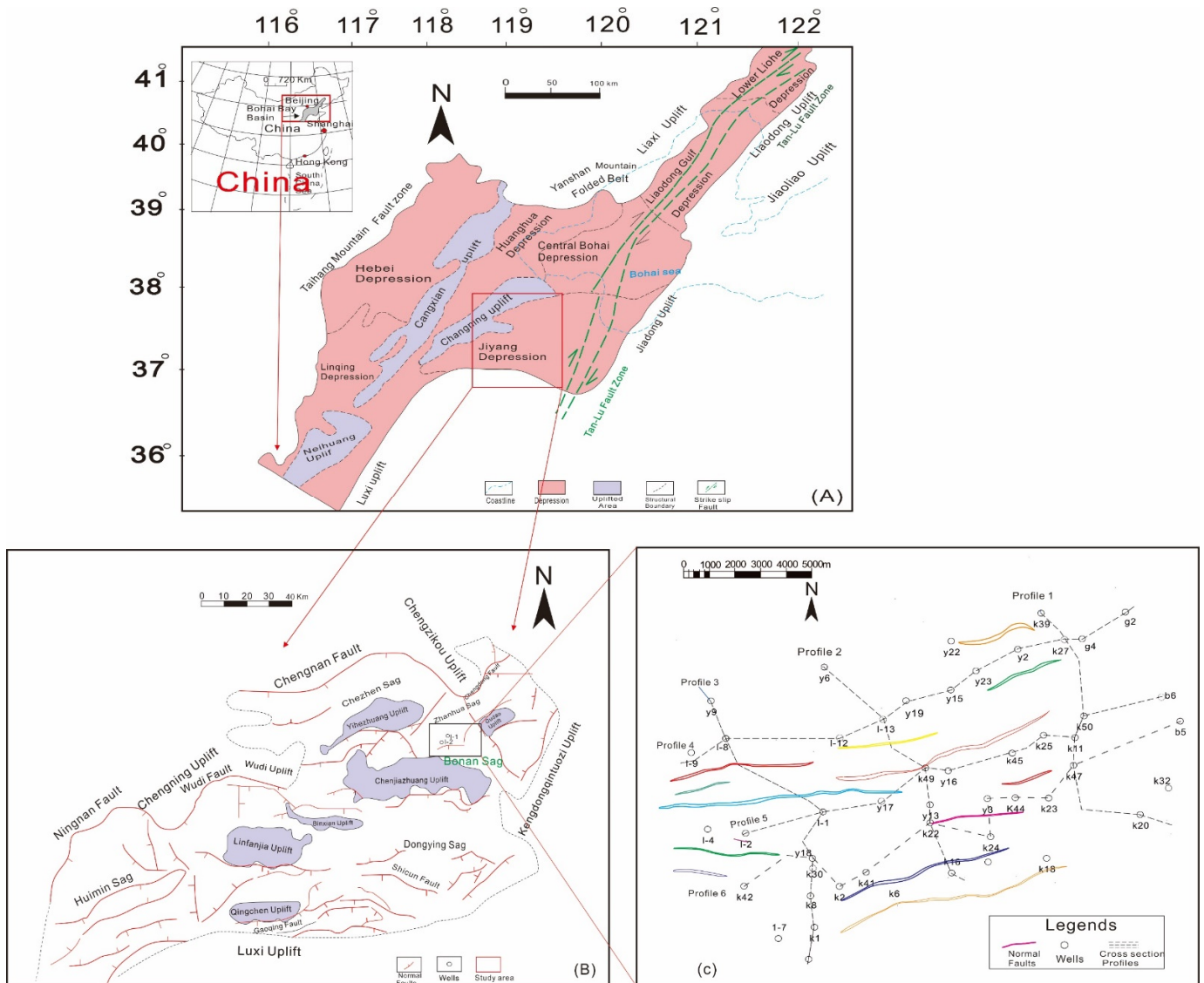

Figure 1. (**A**) Location maps of Bohai Bay Basin in China; (**B**) Structural map of Bonan Sag and associate area; (**C**) location map of the study area with detail seismic and well log profiles.

In the study area, sedimentary rocks were deposited in the syn rifting stage from the Eocene to the Oligocene, which could be further subdivided into two sub-stages. In the initial rifting stage, the Kongdian Formation and the lower-fourth member of the Shahejie formation were deposited; in the later extensional stage, the fourth, the third and the lower-second member of Eocene Shahejie Formation were deposited [17]. During the subsidence, the deposition of the upper second and the first member of the Shahhejie Formation took place [7]. In the second stage of post rifting from Miocene to Pliocene

the upper part (Neogene) and the lower part (Eocene and Paleocene) are separated by a regional unconformity that causes the juxtaposition of Miocene deposits on the Eocene Shahejie formation, and basement faults generated a series of half graben and graben structures [17].The research area is rich in hydrocarbon resources, and their distributaion is present in the Paleogene Shahejie formation, and Neogene Guantao formation. In total, an area of 600 square kilometers had been explored through a 3D seismic survey and there were 377 drilled wells by 2011 in the Bonan Sag [17]. The exploration well density of 0.628 wells per square kilometer was recorded and there was 1.3 billion barrels of cumulative proved oil in place, and it is predicted that there will be 1.23 billion barrels in place [17].

3. Data and Methodology

With the help of cores, log trends and 3D seismic data, sedimentary facies of Es3z sandstone groups in the Bonan sag have been extensively studied for lithology, reservoir's color and facies associations. A total of 78 wells, 23 of which were continuous cored wells, were employed in the modeling software used to probe the detail lithofacies and interpretation of logs. High quality data with no spikes in the caliper logs is used to mark the reliable log information for GR and RT log interpretation. Then, under the guidance of log motifs, gamma ray (GR), spontaneous potential (SP) and resistivity (RT) logs are used to describe facies and lithological characteristics in detail. Cores are used to interpret sedimentary characteristics of sandstone bodies. The middle sub-member (Es3z) is studied here in detail and is divided into a third order sequence, mainly characterized by variegated sandstones from coarse to medium and fine grained sandstone, along with mudstone.

The top (Es3z2+3) and bottom (Es3z8) boundaries of the sandstone groups are regional unconformities and other sandstone groups are bounded in a conformable manner within these boundaries [18]. Sharp lithological contact like truncation of sandstone that underlies the mudstone was kept as a marker bed for the correlation of sandstone groups. Sedimentary facies within each sandstone group was analyzed and correlated within a sequence stratigraphic framework, and the top sand groups act as datum plane, however in order to show the actual steepness profile in correlation, we did not flatten it. Five sandstone groups or units in the third order sequence experienced progradation, retrogradation–progradation, and retrogradation stacking patterns (Figure 2). The Es3z8 sandstone group has a half cycle, in which progradation or a fine to coarsening upward sequence is observed (Figure 2). The complete cycle of retrogradation (coarsening to fining upward sequence) to progradation para sequences (fine to coarsening upward sequence) are interpreted in the Es3z6+7, Es3z5 sand groups, whereas the Es3z4 sandstone group is separated by maximum transgression surface and the Es3z2+3 sand group contains progradation to retrogradations para sequences (Figure 2). Sandstones, mudstones, and siltstones or argillaceous siltstones are found in alternating patterns in reservoir zones (Figure 2).

All core wells were encountered at target depths of required sandstone layers. Depth of the recoverable cores are often matched with the actual value of log at a certain depth. To avoid uncertainty, the depths of cores are carefully checked and regulated by well logs. Depositional facies are described on the basis of criteria defined by Nazeer and Selley (1978) (Figure 3) [19,20] and analysis of gamma ray and spontaneous potential curves that contain different kinds of trends associated with specific depositional environment and facies associations (Figure 3). These trends have been matched in well logs with cores while interpreting the facies and further compared with resistivity logs to maintain accuracy of results. We made different sections in the form of columns for clear interpretation of well logs, sand groups, lithologies, core description and sedimentary facies. Sedimentary facies within each sandstone group are analyzed in terms of lithofacies, facies associations in respective depositional environments. For the clear visualization of cores, we also dispatched core photos in high resolution in separate columns and explained the lithological characteristics, with a description and their interpretation (Table 1).

Seismic data of 100 square kilometers are processed and interpreted, and detailed facies maps are generated through well-seismic analysis to show the facies associations and their distribution in sandstone groups. Thus, the seismic data interpretation is initiated with identifying the horizons in Es3z sandstone groups by utilizing the check shot method. Two sandstone groups, namely the top unit (Es3z2+3) and the bottom unit (Es3z+8), are marked for picking the seismic horizon and other sandstone units bounded between these, which are calibrated with well logs to deduce the sedimentological information in the whole study area. The time-depth relationship at the well was established by a synthetic-to-well tie, which shows the seismic response after comparing it with the actual seismic data. Well data tie in depth domain to seismic data in the time domain will be used to find out events which would ultimately associate with geological formations. The check shot data is only available in well K37, however synthetic seismogram of key wells are constructed.
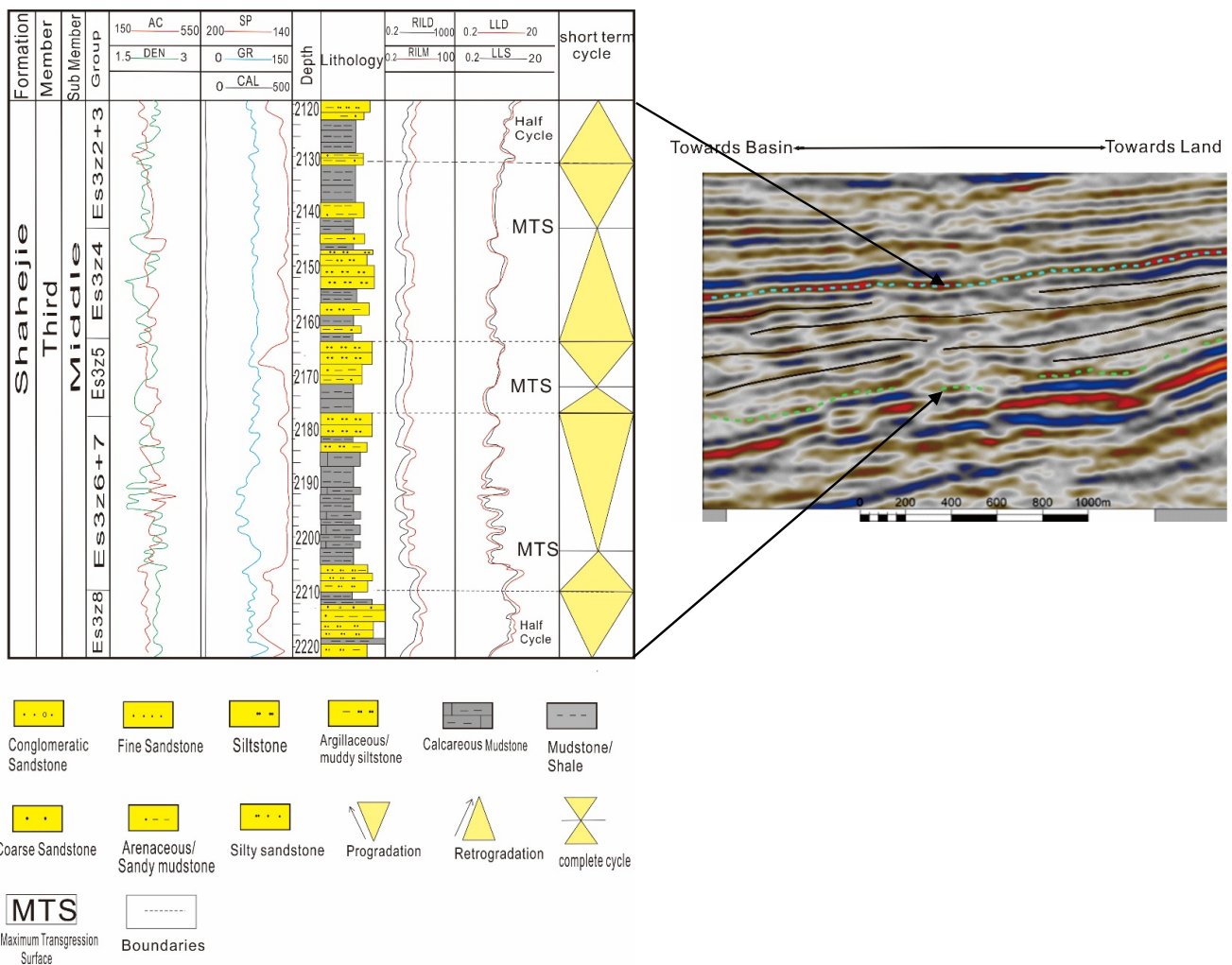

Figure 2. Single well interpretation and representative seismic signals (Well k45) using multiple logs in the middle sub-member of the Shahejie Formation (Es3z), including five groups of sandstones, namely Es3z2+3, Es3z4, Es3z5+6, Es3z7, and Es3z8 in third order sequence. (Top of Es3z2+3 and the bottom unit of Es3z+8 is shown by arrows on seismic). For each group of sandstones, system tracts are recognized by interpreting wireline-log motifs with lithological successions and groupings by (1) sharp lithological contacts (e.g., truncation of clean sandstone with the underlying mudstone or shale), (2) changes in logging curves. Strong negative amplitude (red) marked as sandstone, positive amplitude (grayish) marked as mudstone, area of weak negative amplitude (brownish) siltstone or argillaceous siltstone [18].
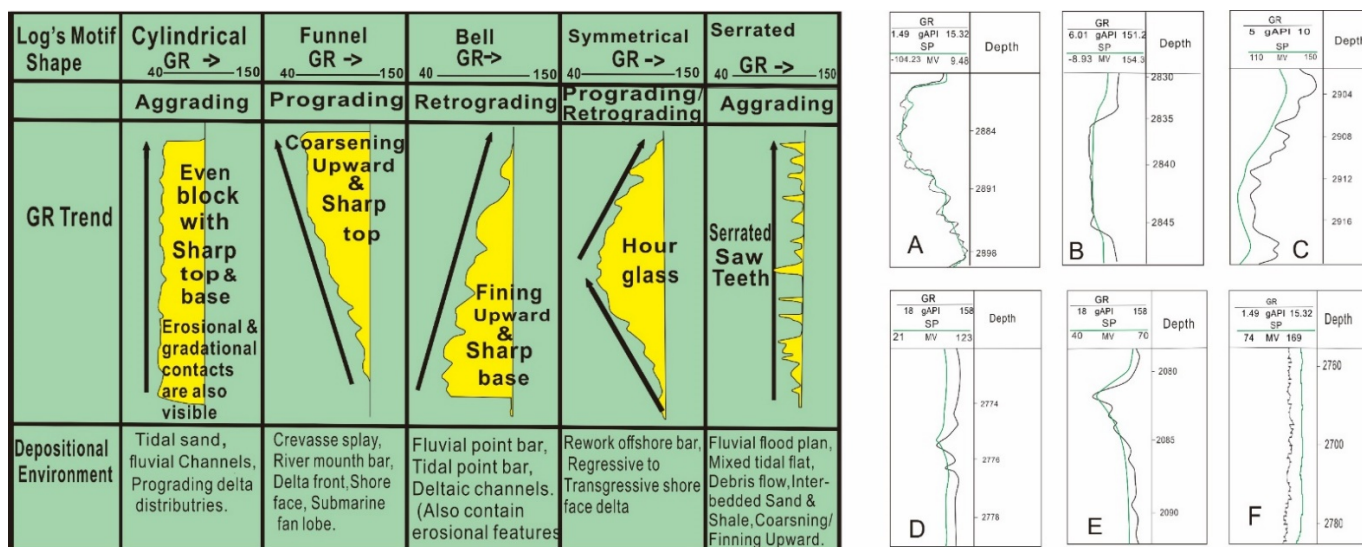
Figure 3. Modified typical trends of gamma ray log shapes at left after Selley and Nazir [19,20], Demonstration of typical logs from study area (**A**) High amplitude funnel-shaped to interpret mouth bars, (**B**) Box-shaped trend to interpret distributary channel, (**C**) Bell-shaped curve for identifying the distributary channel, (**D**) Finger or serrated shaped curve to identify the sand sheet, (**E**) Low amplitude funnel-shaped to recognize the natural levee, (**F**) High amplitude curve to interpret the interdistributary mudstone [18].

Table 1. Representative cores to study lithological characteristics and facies analysis.

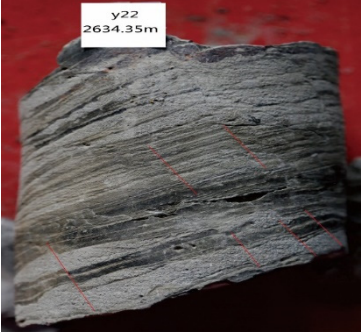| Lithology	Description	Interpretations	Cores
well, k44 Depth:2079.1 Fine silty sandstone	Parallel as well as small scaled cross bedding; siltstone is inversely graded to fine sandstone on the top. Parallel bedding started from siltstone to fine sandstone that turned into a cross bedding structure.	Sand bars migrate in distributary channels, parallel bedding to cross bedding indicate the progradation of delta front facies; a brownish color shows the channel presence in inner delta front deposits of shallow water environment.	
well, k44(C) Depth:2088.75 Massive sandstone	Parallel bedding and small-scale cross bedding; thinner coal bed is embedded in massive sandstone; brownish color can be seen on the top side.	The massive beds were developed under conditions of rapid deposition in the upper flow regime of high-density current. Organic content shows poor oxygenated environments of the inner delta front or delta plain.	

Table 1. *Cont.*

Lithology	Description	Interpretations	Cores
well l-9 Depth: 2659.4 Dark gray calcareous mudstone	Homogenous calcareous mudstone (view from the top); no obvious sedimentary structures are found.	A dark gray or black color shows the sedimentary environment of weak oxidation to reduction in shallow to deep lake; suggested to form in interdistributary channels of the outer delta front.	
Well k45 Depth:2213.85 Light Gray silty sandstone	Wedge shaped cross bedding with an erosional base; cross bedding is also occurring.	This type of bedding is interpreted in high energy environments in the channels. Erosive beds form a wedge shaped structure. It is interpreted to occur in delta front deposits.	
Well Y22 Depth:2634.35 Interbedded mud and sand	Synsedimentary faults are found and display an en echelon array, parallel beds of mud are present, which are more obvious in the middle portion.	These micro faults are interpreted on deltaic slopes and formed due to normal grown faults that initiate sliding in weak lithologies, and hence it marks a transitional zone between the mouth bar and the sheet sands.	
Well, k50(H) Depth:2116.50 Grayish mudstone	Grayish mudstone with scours at the bottom due to underlying sandstone; it marks the erosive contact.	Grayish mudstone is interpreted to form in wetting-reducing conditions in interdistributary areas; representing periodic flow of water due to rising lake levels in flood events; interpreted to form in the inner delta front.	

Table 1. *Cont.*

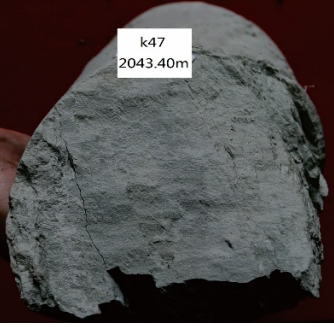| Lithology	Description	Interpretations	Cores
Well k50 Depth: 2163.9 Matrix supported conglomeratic sandstone (MCS)	Mud clasts of grayish color are embedded in these deposits that display a poor sorting, and clasts are angular to sub angular in shape due to less abrasion; showing normal grading and scours are present at the base.	Poor sorting and less abrasion suggested their presence near to sources; interpreted to form in higher energy environments of the inner delta front.	
Well k47 Depth:2043.40 Greenish grey mudstone	Erosion surfaces are found in greenish grey mudstone on the basal side; that marks abrasion with underlying sandstones.	Green mudstone is interpreted to form in wetting-reducing conditions in interdistributary areas; representing periodic flow of water due to rising lake levels in flood events; interpreted to form in the inner delta front.	
Well l-8 Depth:2603 Gray siltstone	Carbon bearing parallel bedding at the bottom; mark a sharp contact with underlaying fine sandstone.	Carbon's presence is Interpreted in low energy reducing environment in distributary channel deposits; stronger wave action influences the grain size in shallow to deep water of outer delta front origin.	
Well l-8 Depth: 2605.4 Fine sand stone	Fine sandstone with ripple parallel lamination; climbing ripples at the bottom; Lamination cover is of dark mud.	Ripple parallel laminations are interpreted to form in a low energy subaqueous reducing environment as mouth bar deposits; stronger wave action in shallow to deep water suggests their occurance in the outer delta front.	

Table 1. *Cont.*

Lithology	Description	Interpretations	Cores
Well k49 Depth: 2340.9 Fine grained gray-brown sandstone	Medium to fine grained gray-brown sandstone; oil bearing scour surfaces at the bottom, normally graded, with a fining upward trend.	Well sorted grains represent the wave action in channel deposits, away from the sources; hence, they are suggested to occur in the outer delta front area.	k49 2340.9m
Well k45 Depth:2215 Silty sandstone	Ripple cross lamination (red lines) at the base of silty sandstone, with erosional structure at the basal side. It shows a good sorting.	Good sorting and ripple cross lamination represent the occurrence of these deposits in the outer delta front area, lower part may contain mouth bar deposits.	k45 2215.35m

4. Results

Five types of facies associations (distributary channel, natural levee, mouth bar and inter-distributary channel, and sheet sand) are recognized in the reservoir intervals, and their identification is based on color, log curves, grain size and sedimentary structures.

The calibration of core photographs with the well log's trend is very important as it reduces uncertainty for interpreting the sedimentary features. In this context, sedimentary features in the Es3z reservoirs are carefully calibrated with log's trends of gamma ray (GR), spontaneous potential (SP) and Resistivities logs (RT). Observations of our study show that Es3z sand groups in the Bonan Sag mainly comprise of Mudstone, muddy sandstone, fine to coarse sandstone and conglomeratic sandstone.

4.1. Mudstones with Associated Sedimentary-Lithofacies Analysis

Horizontal bedding may occur in mudstone, but most of core intervals show massive and structureless features with variable colors, depending on their depositional settings (Figure 4). SP and GR values are observed to be higher as a result of the presence of radioactive elements in shale. However, resistivity log values are generally decreased due to the electrically conductive nature of the mudstones, but for sandstones it shows an almost straight smooth curve of lower GR values. Interdistributary channels are interpreted to occur in between the distributary channels. Grayish mudstone (GM) in inter-distributary channels is shown in the core interval at 2166.50 m in K50 with higher GR values, whereas light to dark grey matrix supported conglomeratic sandstone (MCS) with mud clasts lies in distributary channels of inner fan delta front deposits, containing a matrix of sand and clay (Figure 4). These deposits show a poor sorting, and individual beds have approximately 4 m thickness, shown in the interpreted sedimentary profile, and clasts are angular to sub-angular in shape with normal grading (Figure 4). Clasts have a perpendicular orientation,

and the matrix's geometry suggested that these are transported and deposited together (Figure 4). Medium grained sandstone is also intercalated within individual beds, and scour surfaces are usually present at the base of these deposits (Figure 4). Clast supported conglomeratic sandstone is differentiated from (MCS) by small gravels that are usually interconnected and rounded to sub-rounded or sometimes angular in shape (21). Sandstone has erosion at the basal side. Over all coarsening upward cycles were characterized by conglomeratic sandstones with intercalation of medium grained sandstone at nearly constant values on GR, SP and RT logs and marked gradational contact with facies of interdistributary channels. Gray sandstone has lower GR values but RT logs show the same constant trend for sandstones (Figure 4).
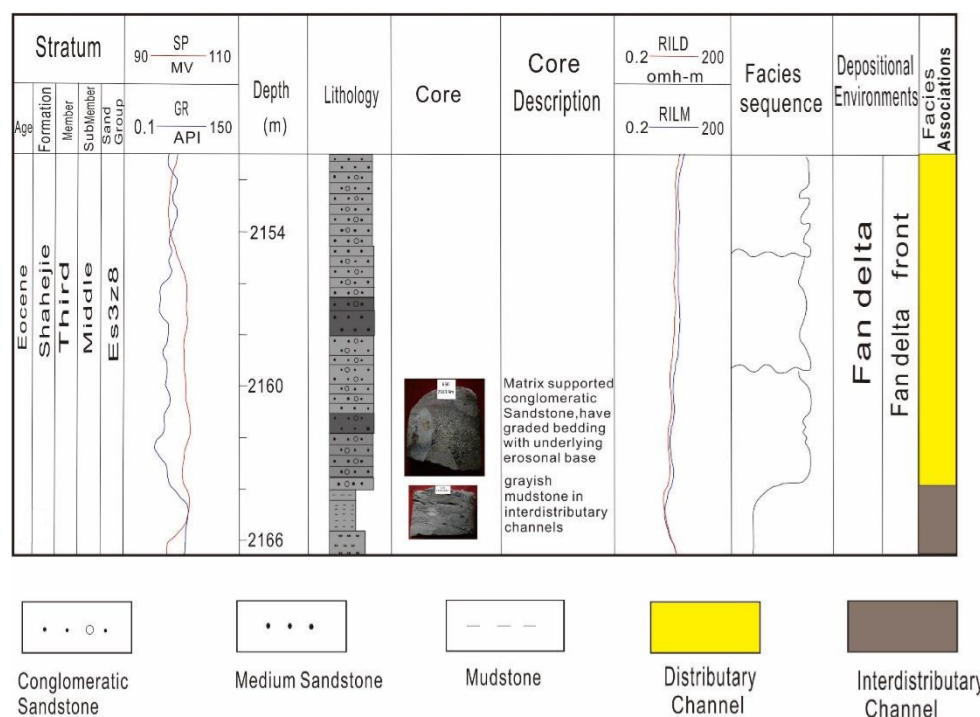

Figure 4. Core well k50 in the study area illustrating facies of the Inner fan delta front, rep resenting trend of log suits with lithology, core, and sedimentary facies. Cores of those dispatched are shown in (Table 1).

4.2. Siltstones with Associated Sedimentary-Lithofacies Analysis

Siltstones are associated in definite proportion with claystone and sandstones. In cores, parallel as well as convolute beddings are observed in delta-front deposits (Figure 5) [9]. Parallel bedding are sometimes interpreted as horizontal bedding.The parallel and horizontal beddings are distinguished on the basis of laminae, and the former is less than one centimeter, indicating a high-water energy depositional environment. Convolute beddings formed on slopes due to shear stress in sand to silt size particles. It also appears in cross laminated sediments after deformation and has turned into small scaled anticlines and synclines structures [9]. Convolute bedding is commonly observed in the Es3z sub-member, and it is considered to be formed soon after deposition in siltstones [9]. As these deposits are interpreted to occur at the outer part of delta front in clinoform's areas in the higher slope, they can also be formed in shelfal lobes. The corresponding log values are changed due to a variation in shale and sand contents in sheet sand (Figure 6). On GR log, middle to high amplitude values of serrated shapes are observed. Soft sediment deformation is also observed in natural levee deposits, and mostly sharp peaks are detected at the topmost part of a coarsening upward sequence with lower to medium GR log values (Figure 5A). Natural levees are found on both sides of distributary channels, and considered to be formed when channels deposits are overflown on the bank sides due to a flooding event.

Besides convolute bedding, deformed bedding is common in siltstones (Figure 6A). It showed deformation in soft sediments with high dip angles as shown in the figure below (Figure 5A).
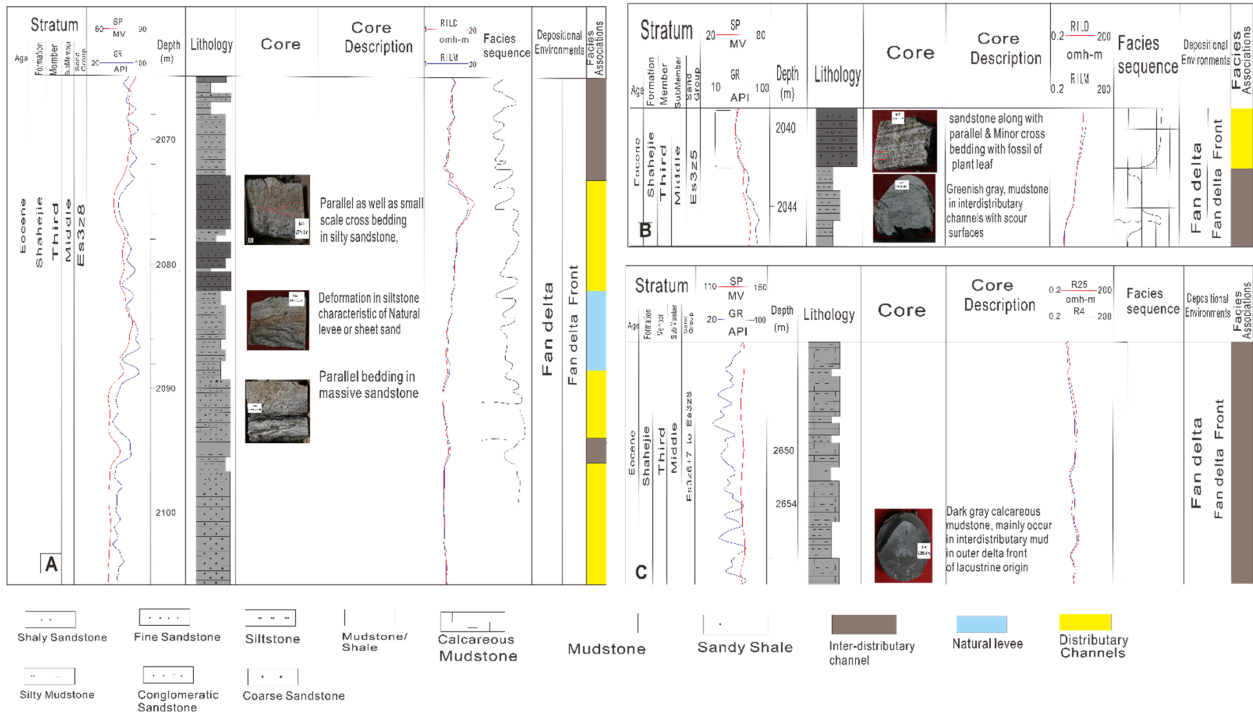

Figure 5. (**A–C**) Core wells k44, k47 and l-9 in the study area, representing trend of log suits with lithology, core and sedimentary facies. Cores of those dispatched in (Table 1).
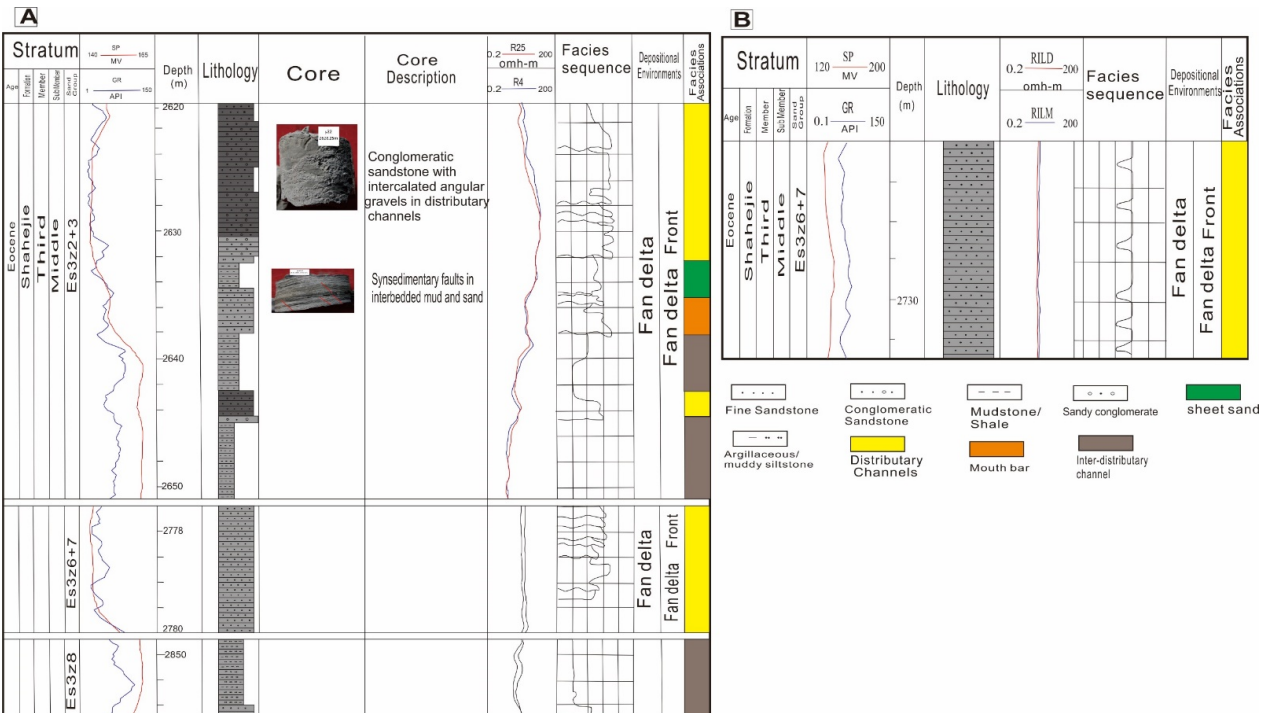

Figure 6. Core wells Y22 (**A**) and y23 (**B**) in the study area, which shows trend of log suits with lithology, core and indication of sedimentary facies. Cores of those dispatched in (Table 1).

As described above, siltstones are associated with sandstones that are described in Figure 5, in which lower GR values of Box shaped with parallel as well as small scaled cross bedding in silty sandstone (PCSs) are interpreted at the depth of 2070.1 m in well k44 (Figure 5A). It is considered to be formed in distributary channel deposits, the thickness of which varies up to 4 m (Figure 5A). It marks a sharp contact with facies associations of interdistributary channels, and displays a fining upward trend on the top (Figure 5A). Deformation in siltstone (DS) is also found in natural levee deposits with rusted color at 2087.9 m in well k44 where siltstone is inversely graded into sandstone on the top. On the basal side, parallel bedding in massive sandstone (MS) is interpreted in channel deposits at the depth of 2088.75 m that shows the box shaped curve on GR log (Figure 5A).

To describe the characteristics of the delta front, box shaped sandstone along with dominant parallel and minor cross bedding in coarse grained sandstone (PBCs) are found at the depth of 2041.85 m in well k47. (Figure 5B). Plant leaf is also seen, which shows its presence near to sources (Figure 5B). As delta prograde it forms a shallowing up pattern that contains younger sediments deposited in shallow water with overlying coarser sediments (Figure 5B). In the wet tropical climate vegetation that covered the delta top or delta front, and over the bank, flood transports the beds further into inner part of the delta, which preserved the relics of vegetation in the form of roots or plant leaf (5B). Beside sandstone, Greenish gray mudstone (GGM) is interpreted to lie in inter-distributary channels with higher GR values with erosion at the basal side and sharp contact with the sandstone on the top, and it does not display any sedimentary structure due to less wave action and the fact that their deposition is near to sources (Figure 6B). Conversely, dark grey mudstone (DGM) with calcareous content is interpreted as inter-distributary mud in the outer delta front of lacustrine origin (Figure 5C). During transgression, mudstones are overlying on coarse grained beds of channel deposits. For lacustrine mudstone, GR log shows a constant sinusoidal curve, and SP log has higher values in well l-9 with no obvious sedimentary structure.

4.3. Sandstones with Associated Sedimentary-Lithofacies Analysis

During the investigation of cores, different textures of sandstones are found in the Es3z sub-member, including matrix supported sandstone with underlying scoured surfaces, conglomeratic sandstone (Figures 4, 6 and 7), massive sandstone, coarse grained sandstone, medium grained sandstone (Figure 6), and fine sandstone (Figure 8). The fine-grained sandstones are categorized with low amplitude, box-shaped curves on GR log, with lower resistivity values. It contains symmetrical wave ripple parallel lamination and interpreted in fine sandstone that is evidence of matrix free sandstone (Figure 8). Wave ripple parallel lamination is often formed in shallower water by oscillatory motion in the water column due to absence of high currents [21] (Figure 8). Due to the migration of ripples, and sand waves, most of the cross beds are formed [21]. All these structures are interpreted in the Es3z sub-member except tabular cross bedding.

Medium to coarse sandstones, conglomeratic and massive sandstones have a boxed shape on GR log with lower to medium amplitude values, trending from coarsening to the fining upward. Parallel bedding, and cross bedding are found in these deposits (Figures 4 and 5). Conglomerates are associated both with mudstones and sandstones in the study area, representing a high energy environment and are found in channel deposits. Sometimes these deposits exhibit scour surfaces that indicate the erosion of sediments on the basal side, and it is not associated with any lithology. These are found both in mudstone and sandstones of the Es3z and occur when coarse grained sediments overlay the scour surfaces (Figures 4 and 5). Box shape trends of distributary channels are shown in (Figure 6), which display lower GR values, and are interpreted to have inversely graded conglomeratic sandstone (CSg) with intercalated angular gravels (mud clasts) at the depth of 2628.25 m in well Y22. Basal contact of (CSg) has gradational contact with sandy conglomerates (Figure 6) that turns into interbedded mud and sand at the bottom (Figure 6). As we move towards the basin side, synsedimentary faults (SSM) are found at the depth of 2634.35 m

in well Y22, particularly in those lithologies in which muds and sands have alternate parallel layers, and are interpreted as sheet sand deposits due to the corresponding log showing a serrated shape (Figure 6). These micro normal faults appear on deltaic slopes and are suggested to occur as a result of the normal growth faults, which cause sliding in weak lithologies.

Sheet sands are associated with the mouth bar deposit that shows a coarsening upward sequence in the fine sandstones (CFs). (CFs) marks a sharp contact with sheet sand on the top, and interdistributary mudstones are present at the basal side, which grades into 2.5-m box shaped sandstone at the lower contact that is followed again by mudstones towards the bottom (Figure 6). The same trend of box-shaped is interpreted in other sandstone units, which contain fine grained sandstones in distributary channels (BFS) (Figure 6). Interdistributary channels also contain argillaceous siltstones that are evident from the GR and SP log (Figure 6).
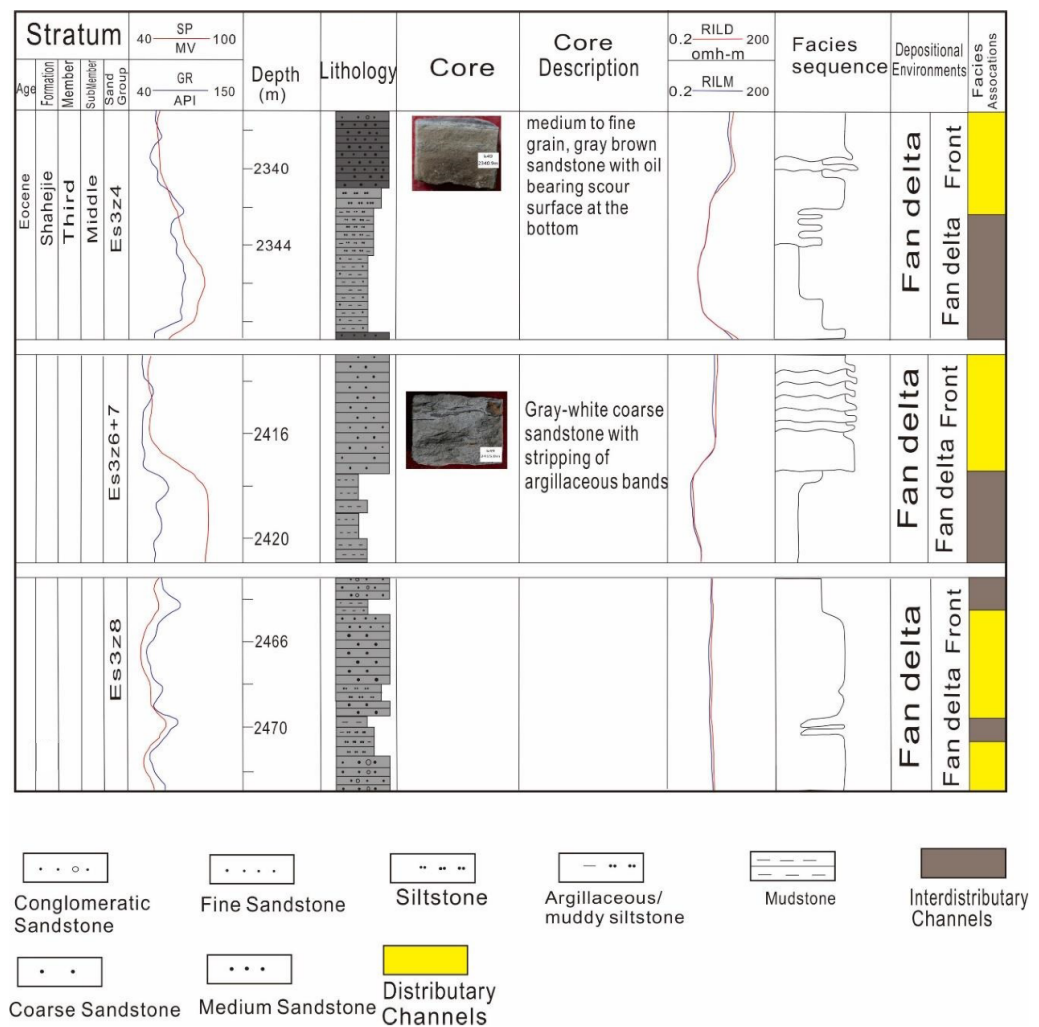

Figure 7. Core wells 49 in the study area, which shows trend of log suits with lithology, core and indication of sedimentary facies.
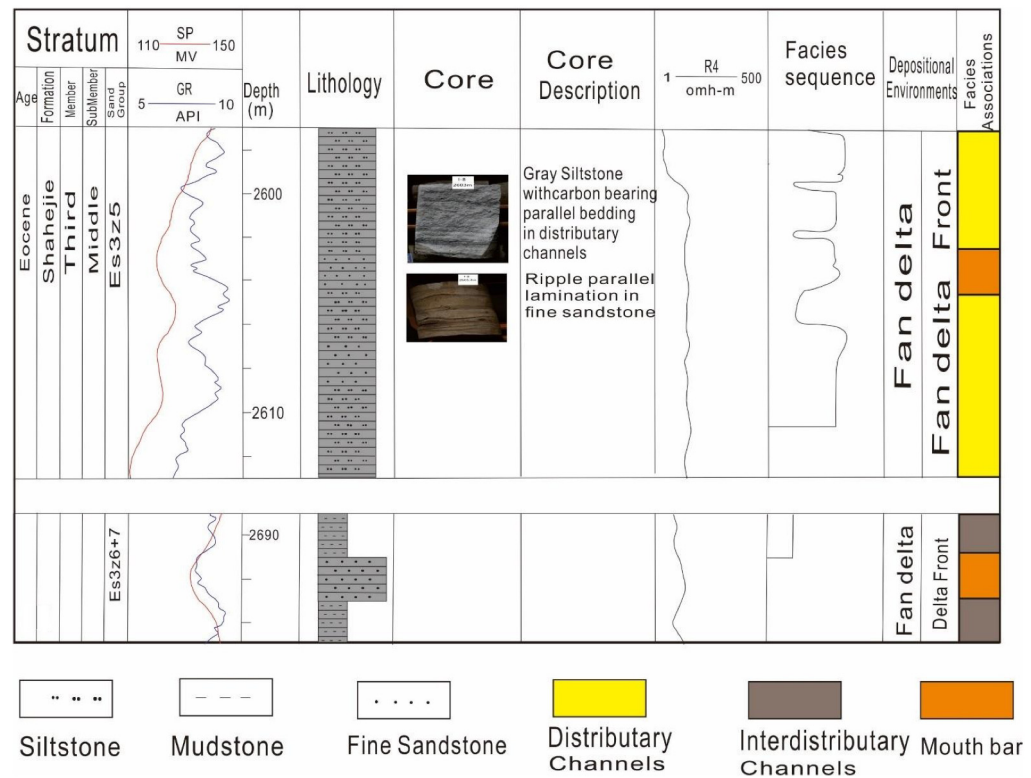
Figure 8. Core well l-8 in study area, showing the trend of logs suits with lithology, core and sedimentary facies.

As described above, sandstone units have different textures. From core studies, gray brown oil bearing fine to medium grained sandstone along with scour surface is seen at the depth of 2340.9 m in well k49 (Figure 7). From core and seismic analysis, these deposits are evident to occur in the slope belt of the outer delta front of the middle area. Overall, a coarsening upward trend is observed in medium grained grayish-brown sandstone (GBS), but the corresponding log shows a boxed shape trend in sandstones (Figure 7). Basal side has gradational contact, which changes into siltstone, argillaceous siltstone, and finally into mudstone towards the bottom (Figure 7). Gray-white coarse sandstones also occur with the stripping of argillaceous bands (rip up clasts) (RCS) at the depth of 2415 m (k49) (Figure 7) in the distributary channels, which have sharp contact with the interdistributary mudstone at the bottom. On GR and SP logs, cylindrical and bell-shaped curves are observed in distributaries and interdistributary channels, however, RT values are higher in the case of sandstones, and lower in mudstones (Figure 7). Coarse grained sandstone intercalated with siltstone layers are also found in the Es3z8 sand group, contain an average thickness of 2 m and mark sharp contact with mudstone, which is the muddy siltstone deposits of interdistributary origin (Figure 7).

As variegated sandstone is found in delta front's depositional environments, fine sandstone was found with a sedimentary structure of ripple parallel lamination at the depth of 2605.4 m in well l-8 (Figure 8). Fine sandstones possess the wave-ripple laminations (PLS) that are evident in (Figure 8). The trend of the gamma ray log is coarsening upward as funnel shaped, and above the mouth bar sandstone, a gray siltstone with carbon bearing parallel bedding (PBSs) is interpreted in distributary channels with bell shaped trending of the GR log curve at the depth of 2603 m in well 8 (Figure 8). Mouth bar deposits have sharp contact with siltstones on the top. Over all, GR log values have a fining upward trend with alternate layers of siltstone, sandstones and then siltstones from bottom to the top (Figure 8). The lower sandstone units of Es3z6+7 also consist of fine sandstones of mouth bar deposits bounded by interdistributary mudstones. Mouth bar deposits have coarsening upward sandstones in all sand groups (Figure 8).

Beside ripple laminations, wedge-shaped cross-bedded silty sandstone (WCS) is also interpreted in distributary channels, and formed in the high energy environment with underlying erosive surfaces (Figure 9). It is a distinguishing feature of sandstone, and on the GR log this coincides with the lower values of the curve, although corresponding RT values are higher. Ripple cross lamination (RCL) is also interpreted in silty sandstone, and due to rapid deposition, ripple cross-lamination is formed (Figure 9). A series of cross-laminae is produced due to superimposition of one ripple on another as the ripples migrate. Fining upward bell shaped parallel and massive crossbedding sandstone (MS) is considered to lie in distributary channels, varying from coarse sandstone to siltstone at the top. Erosive surfaces are commonly seen in the Es3z sub-member. Coarse grained sediments are overlying the scour surfaces. These surfaces are not associated with any lithology or environment but are formed due to high energy currents. Figures 4–7 and 9 illustrate scour surfaces, in which the lower portion of the sediments faced erosion due to sandstones.
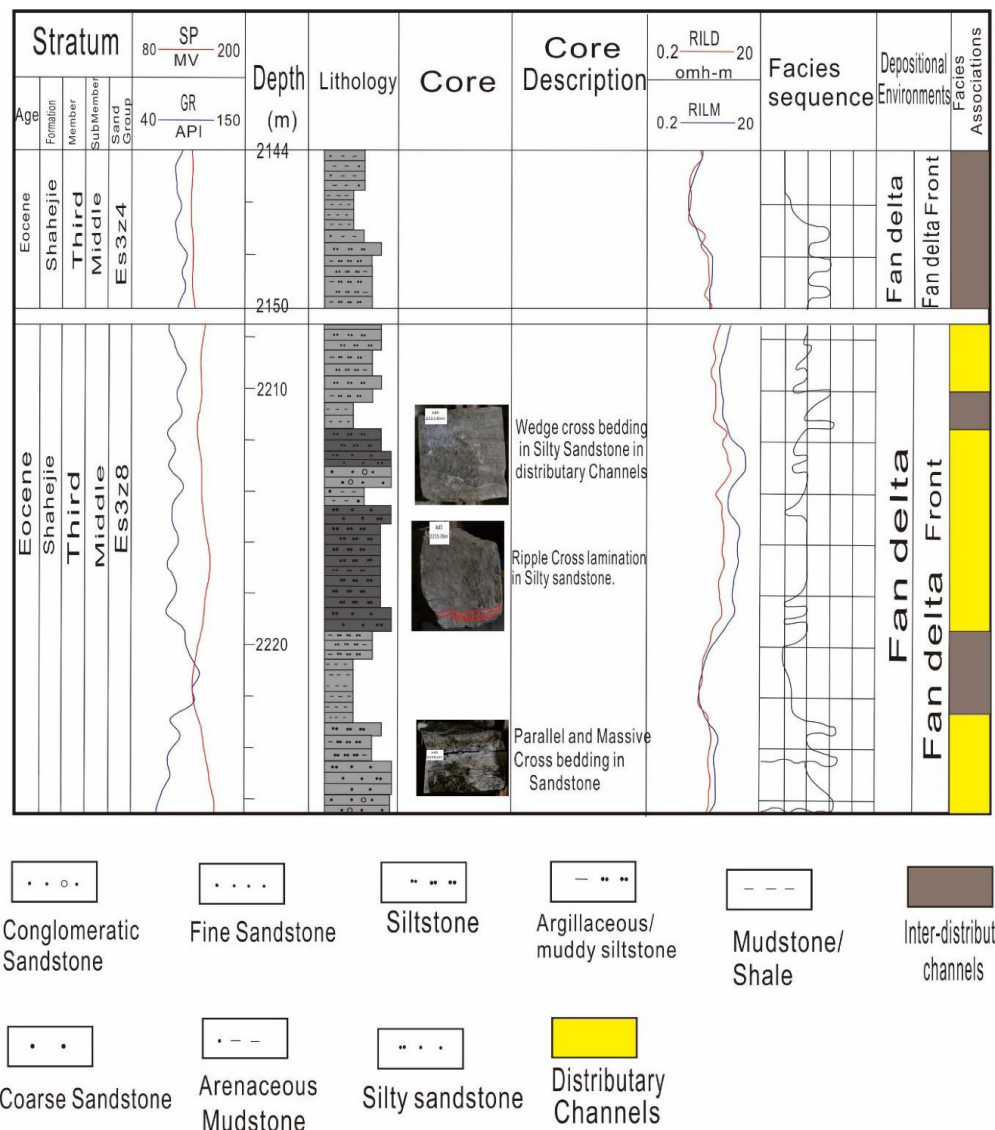

Figure 9. Core wells K45 in the study area with complete set of logs along facies, in which Wedge cross bedding in Light Gray silty sandstone is observed at 2213.85 m; Ripple cross lamination in silty sandstone at 2215.35 m and parallel as well as cross bedding in massive sandstone at depth of 2223.1 m.

We were interested to deduce facies of the Es3z middle sub-member. The seismic section was mapped to figure out the information between the top (Es3z2+3) and bottom (Es3z8) of the sandstone groups (Figure 10). These surfaces have prominent amplitude with erosional surfaces but overall possess good continuity. Representative seismic sections are demonstrated to analyze the facies in south to north, and east to west directions (Figures 10 and 11). Deltaic chloroform's truncation is observed in sandstone units in extensional settings (Figure 10). The above area lies in the clinoform's setting, in which depositional surfaces display a wedge-shaped sloping pattern (Figure 10). The highlighted truncation in Figure 10 demonstrates the clinoform's area, as all reflectors are not parallel and the overall seismic profile displays the wedge-shaped slope region in weak lithologies of fine sandstone siltstones and mudstones in wider beds. Normal faults are also observed, some of layers are separated, and the throw of faults seem to be higher. These faults trigger to move the sediments further towards the basin side in a prograding manner (Figure 11). Three major sequence boundaries were observed with good seismic reflections, and prograding reflectors are bounded between these sequences. Onlap reflection terminations are observed in the lower and upper boundaries (Figures 10 and 11). The negative amplitude of red or lighter red color contains siltstones, sandstones, and argillaceous contents, while mudstones are presented as positive amplitude that are lighter gray in color (Figure 11). Whereas brighter reflections are considered to have conglomerates in sandstone bodies. Argillaceous content increases along with silty content when the velocity of channels are reduced and sediments are deposited on distal sides, which is shown both laterally and vertically (Figure 11).

Seismic reflection pattern is interpreted as parallel with over all high amplitude values at the top and the bottom (Figure 11). Toplap and onlap truncations are also visible that clearly mark on Es3z2+3 and Es3z8 sequence boundaries (Figure 11). Progradational reflectors are interpreted in both continuous and discontinues manners, which are interpreted to be occurring on the steep slopes of basin controlling faults in the fan delta front (Figure 11). Just as the seismic profile from south to north, the stratal thickness increased towards the basin at the western side (Figure 11). Fine to medium grained sandstones, siltstones and mudstones are found on the outer side of the delta front shown in cored wells k45, k49 and seismic profiles depict medium to weak seismic reflections (Figures 7, 10 and 11). Conversely, we found a strong reflections pattern in well K11 near to the source area in core well k50, in which distributary channels contain blockier deposits and are considered to lie in the inner delta front region. Interdistributary channels are suggested to have weak amplitude values, and are demonstrated as a grayish color in the seismic reflection pattern, mostly in mudstones or shales (Figure 11), while brownish reflectors contain siltstones and sometimes grayish and brown reflectors appear together, where siltstones are associated with shaley contents. On the other hand, sandstones show a strong reflection, mainly in the form of prograding black reflectors. With vertical facies associations, mainly distributary and interdistributary channels are interpreted, and they possess a repeatable succession of sandstones, siltstones, and mudstones, which is the diagnostic feature of deltas (Figure 11).

To further testify our results for correlation of the regional sequence boundaries, a synthetic seismogram was constructed in four key wells, and calibrated with the actual seismic profiles across the whole area (Figure 11C). Seismic to well tie was completed by utilizing sonic log, density log, and well tops. The densities and velocities of sand groups are used to create reflection coefficients, which are further convolved with a Ricker wavelet of 40 Hz to generate the seismic signal of respective sand group. Furthermore, results are compared with the seismic horizons. The horizons are picked by synthetic seismogram; the top and bottom horizons are picked for correlation. The boundaries of other reflectors in sand groups display a good calibration with the prominent amplitude of a synthetic seismogram, which shows good agreement (Figure 11C). These sandstone groups have prominent prograding reflectors, which are oriented towards the basin side. Seismic-synthetic calibration in wells K11, K45, K49 and K17 also shows the lateral vari-

ation in thickness of sand bodies, displaying maximum thickness towards the basin side (Figure 11C).
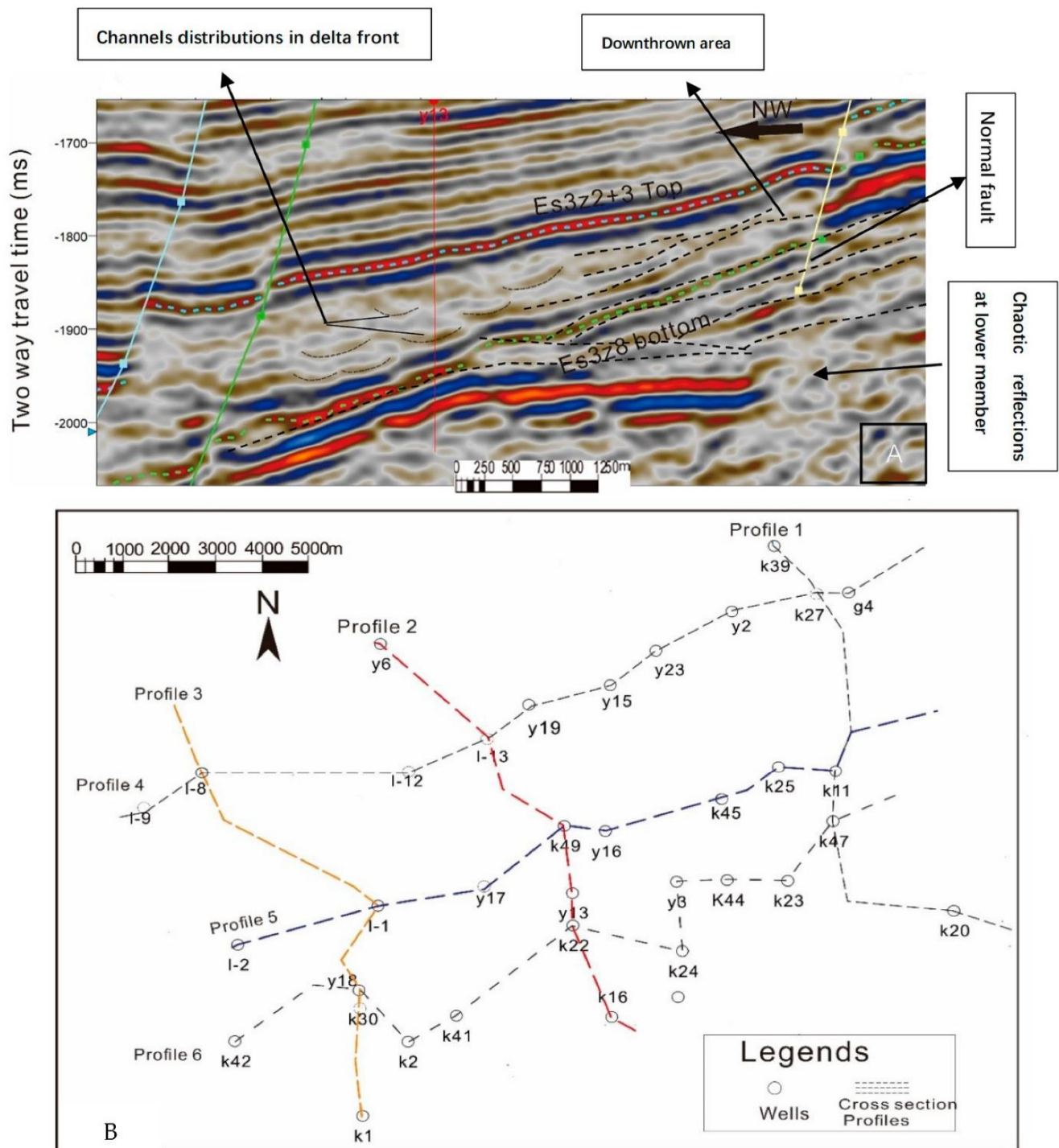
Figure 10. (**A**) Representative seismic section, seismic response of the channels along profile. Prograding reflectors on the deltaic slope belt, top and bottom of sandstone units are visible to be mapped, (**B**) seismic profiles of location area.

Figure 11. (**A**) Eye shape reflections, marked as fan delta front deposit from east to west profile (seismic profile 5 of location area in Figure 10). (**B**) Calibration of seismic with GR logs in key wells (**C**) Synthetic seismogram generation in key wells (Profile 5 shown in Figures 1 and 10).

5. Discussion

5.1. Depositional Facies Analysis

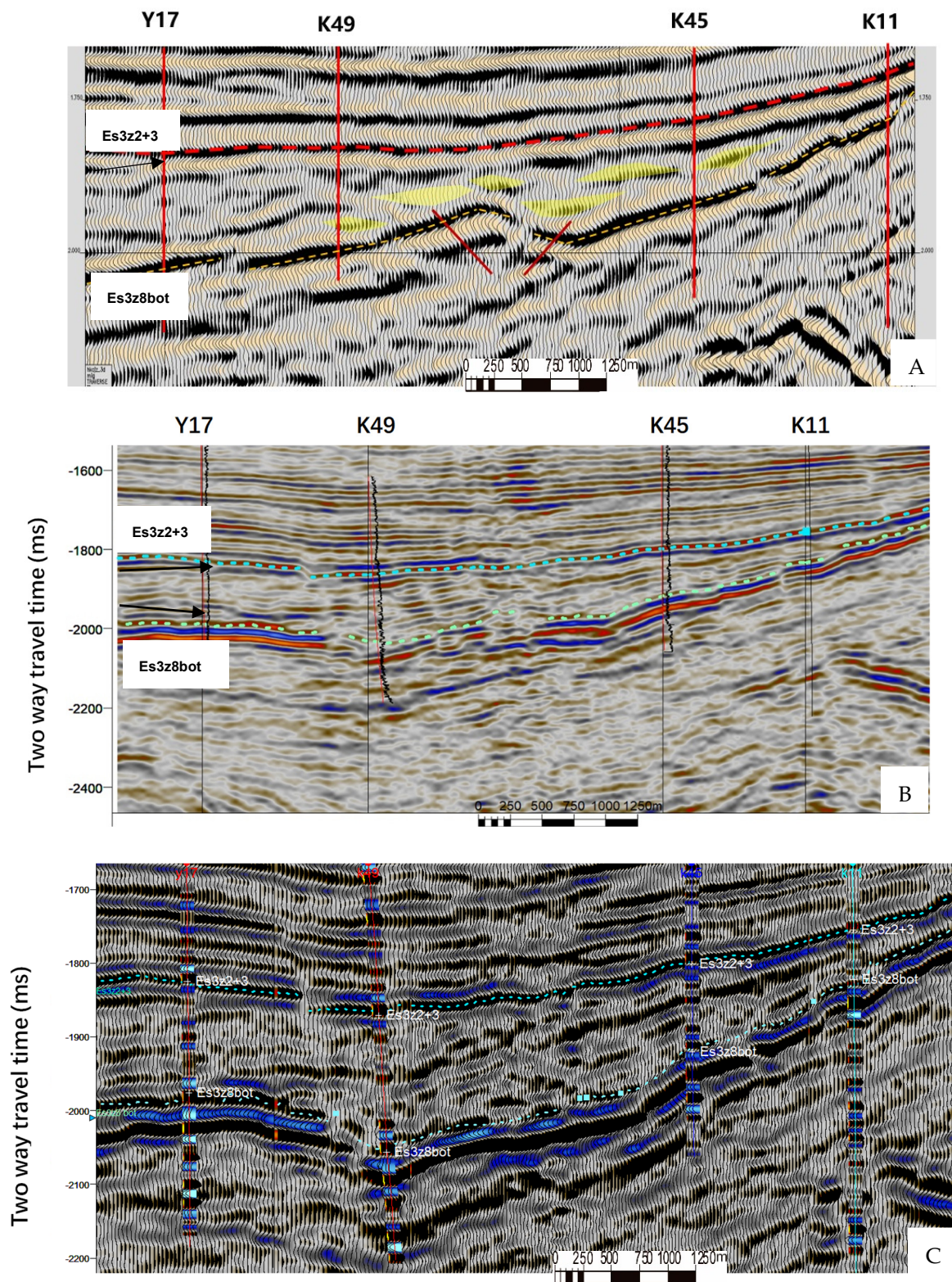GR, SP and RT logs were mainly analyzed, and linked them with seismic data, well logs and core sedimentology in order to recognize depositional facies and lithologies in Es3z sandstone groups. On seismic, facies within the depositional setting of the fan delta front are identified and furthermore, with integrative studies of seismic, wells and cores, five facies associations are interpreted into five sandstone groups in midterm cycles, which mainly lie in the deltaic system (Figure 2).

The delta front is divided into inner and outer components. Facies associations recognized in the inner and outer fan delta front within the five sand groups namely: Es3z2+3, Es3z4, Es3z5, Es3z6+7 and Es3z8 units that have never been defined in detail by previous researchers [3,7,22–24]. As the Es3z shows a second-order sequence that is mainly characterized by variegated sandstones from coarse to medium and fine grain along with mudstone (Figure 4) [5,7] but with lithology, detail facies analysis of sandstone groups in the Es3z sub-member has been less discussed in previous studies except for the overall stratigraphy and facies of the third sub-member of Es3 [25,26].

Inner delta front is characterized by facies associations of distributary channel sandstones, and narrow levees and inter-channel mudstone. The grain size of channel sandstones in the inner delta front is relatively coarser than those characteristics of the distributary channels of the outer deltaic front as these lithologies lie near to the source areas (Figure 4). Sandy and thick coarsening upward successions such as mouth bar deposits are lacking in the inner delta front. The color of the coring interval is shallow gray, which is less dark than the outer delta front deposit. The color of mudstone in inner delta front is lighter than the dark mudstone of the outer delta front (Figure 5).

The outer delta front is characterized by facies associations of distributary channels, mouth bar, levees and sheet sandstone. Typically, the mouth bar deposit contains sandy and coarsening upward successions. Mudstones in interdistributary channels have greenish gray or darker color, and distributary channels are less blocky as compared to the channel deposits of the outer delta front (Figures 5B,C and 8). The overall deposition of sand in the delta front is controlled by a lake or river [27], and these factors have an influence on the depositional setting in our study area. We found lacustrine mudstone in the outer delta front deposits, which is characterized by facies associations of inter-distributary channel deposits, and we can distinguish it on the basis of the color being dark gray calcareous mudstone (Figure 5C).

Distributary channels in the study area were found in the fan delta front. The main lithological associations are medium to coarse sandstones, conglomeratic sandstones, massive and silty sandstones. Fine sandstone and siltstones with parallel bedding are also seen in distributary channels (Figure 8) that indicate low energy subaqueous reducing environment due to stronger wave action and their presence in shallow to deep water [28,29]. Generally, for major distributary channels, sediment supply has a stable path for transportation [30]. Conglomerates bearing poorly rounded clasts usually occur in channel deposits of the inner delta front and indicate high energy conditions of the submerged environment. Parallel, wedged shaped and cross bedded sandstones with scour surfaces, exhibiting box-shaped or bell-shaped trends are interpreted as distributary channel depositions [30,31] (Figures 4–9). Cross bedding occurs in a wide range of patterns including ripples, trough, tabular as well as wedged shapes, which show the direction of water flow along the slope of lee surface (Figures 4, 5, 8 and 9). The massive bedding and scour structures are interpreted as being representative of distributary channel deposits, indicating the condition of rapid deposition in upper flow regime, and was matched with the work done by Van et al., 2015 [32].

Overbank sand is formed during flood events, when sediments from channels are over flowing and deposited at the bank side as a natural levees [21]. A sharp peak in the coarsening upward trend was interpreted as a natural levees deposit and lie adjacent to distributary and inter-distributary channels (Figure 12). Deformed reddish siltstones

represent a natural levee in hot and dry paleoclimatic conditions. We can distinguish natural levee from mouth bar on the basis of available core and the trend of the log, which is obviously sharper in the case of mouth bar deposits, however, sheet sand has a serrated curve with no obvious trend of fining and coarsening upward. It also depends on lithology with more abundance towards the basin.
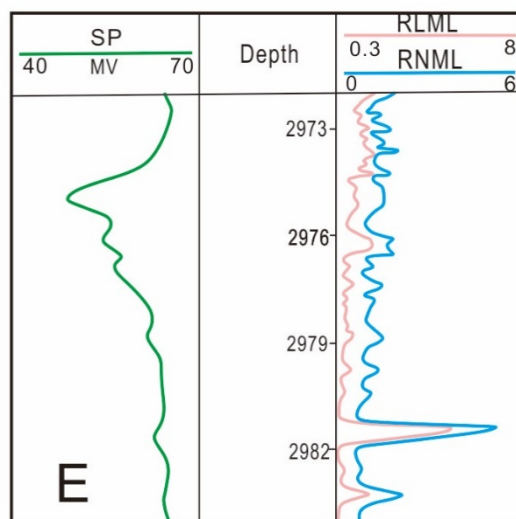

Figure 12. Demonstration curves of natural levee deposits using multiple logs in the study area.

Distributary mouth bars in the research area have obvious coarsening upward trends or funnel-shaped curves on gamma ray logs with lithology grading from silty sandstone or fine sandstone to a thicker bed of sandstone (Figures 6, 8 and 9). At base of mouth bars, thin levels of siltstones or sandstones occur, while thicker beds characterize the top of sandstone [9] (Figures 6, 8 and 9). These deposits have low contents of mudstone and sometimes mouth bar deposits are superimposed by distributary channels when delta prograde [33,34]. In some cases, the grain size appearance of the mouth bar deposits is similar to distributary channel sandstones due to wave action in the outer part of delta front, however, we can differentiate it on the basis of the GR logging curve having a funnel shape or coarsening upward succession. Sedimentary features like a small amount of wave ripple laminations are observed in cores (Figure 8) that make an agreement with previous interpretation by (Li et al., 2014) [30]. Ripple cross-lamination in siltstone and fine-grained sandstone may also represent distal bar or mouth bar deposit when GR log displays a coarsening upward trend, but in the study we found serrated box-shaped with higher GR values (Figure 9) [9].

The inter-channel environments in the delta are marked by: (1) the color and composition of mudstones, and sometimes it comprises of muddy siltstones; (2) High gamma ray log values related to the presence of shale, and no obvious sedimentary features are found in inter-distributary deposits. Interdistributary mudstones lie between distributary channels, and these interbedded mudstones are structureless and mostly contain smooth curves on the GR log. Scour surfaces can also be observed in mudstones due to overlying sandstones (Figures 4 and 5). On the GR log and in the core investigation, cross bedded sandstones turned into mudstone on top with decreasing RT values [9], however, in the study area interdistributary deposits are associated with all kinds of sandstones. Mudstones in the delta front also contain a mauve color when the water level of a shallow lake is changed, and the oxygen concentration in the water increases.

Convolute bedding is a diagnostic feature of sheet sandstone [30]. It is distinguished from mouth bar deposits by the occurrence of thinner sandstone or siltstone [35]. Sheet sand occurs in the outer delta front deposits (Figure 13). Convolute bedding forms, when sediments are deposited on inclined slopes and are subject to shear stress, and this kind of soft-sediments deformation structure affects siliciclastic sediment from fine sand to

silt sized, and produces small scale antiforms and synforms [21,36,37]. Sheet sand has gone through the process of slumping, and such kinds of deformed beddings are often interpreted in these deposits. Generally, sheet sands contain a serrated shape on the GR log and can also be formed in soft sediments due to tsunami, seismic activity and storms [38–40]. Convolute bedding and syn-sedimentary faults are found in sheet sands in the study area (Figures 6 and 13).
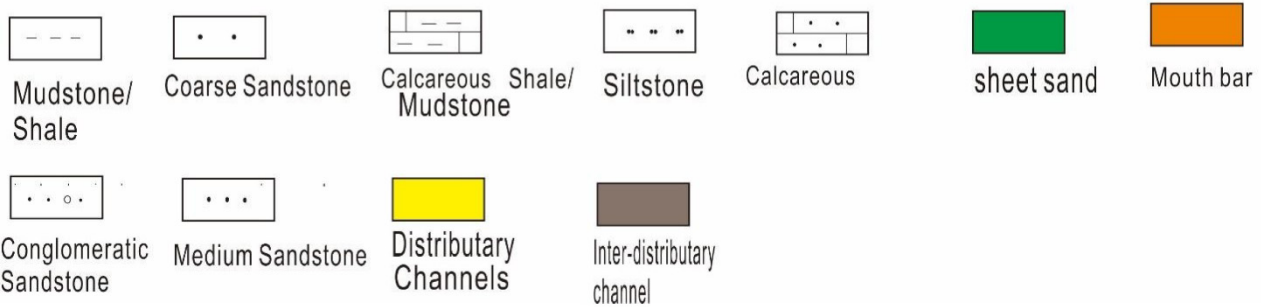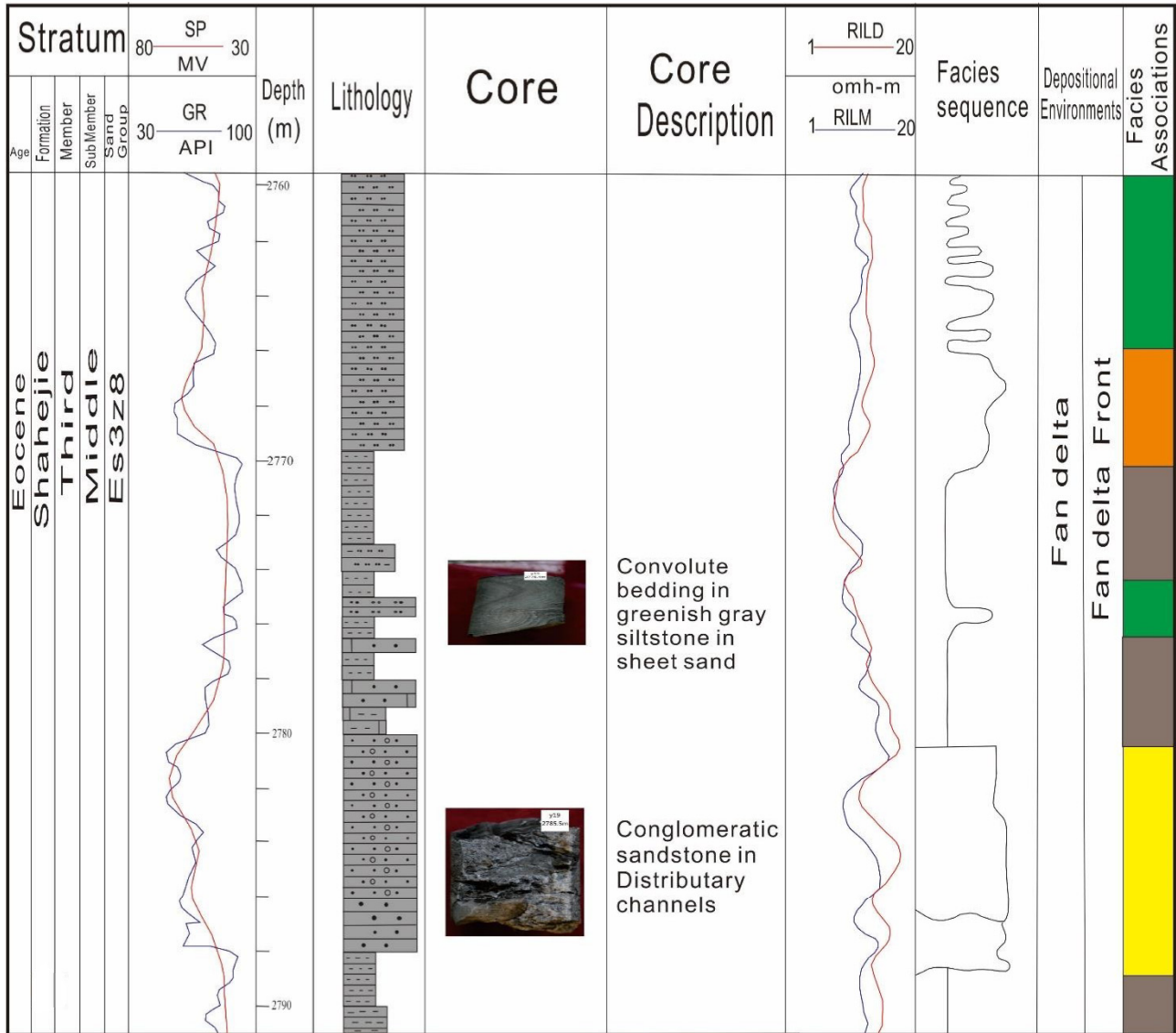

Figure 13. Core well Y19 in study area; convolute bedding in greenish gray siltstone (CBS); conglomeratic sandstone in distributary channels.

The distribution of the inner and outer delta front facies is also recognized through the interpretation of seismic profiles from south-north to east-west, and by comparing them with cores and well logs. Emplacement of the Es3z sand groups were controlled by the topography of the area, bearing growing gradients moving from south-east to north-west. Steepness increased with gradient. From seismic profiles, steepness is interpreted to become an increase in the basin ward, and fine sandstones of distributary channels and mouth bars were deposited on the outer side of the delta front (Figures 8, 10 and 11). Whereas coarse grained deposits are interpreted to occur at the south-eastern part near to sources. The steepness and lithologies marked a zone between the outer and inner delta front. From 3D seismic profiles and cored wells, outer and inner delta fronts showed a substantial variation in vertical and horizontal sedimentary facies of different lithofacies successions. Sedimentary facies and lithofacies show a shallow thickness in the south-eastern part of the study area, and thickness increased towards the basin (Figures 10 and 11). Mudstones in the delta front showed low amplitude values with distinct colors of light gray, green and dark features in reduction and oxidation stages (Figures 10 and 11)

Channel and mouth-bar deposits in the deltaic secession are considered very important from an exploration point of view due to their isolation and being trapped by the delta plain and prodelta mudstones both vertically and horizontally, so they can be an excellent stratigraphic trap. Channels provide a complete system for continuous transportation of hydrocarbons. The reservoir potential of distributary channels is different from fluvial channels, therefore careful interpretation is required for their identification, which leads to the attainment of beneficial exploration and development results. The quality of the seismic data in other sandstones possess the information of weak amplitudes, which was improved by constructing a synthetic seismogram, although the top and bottom of sand groups were clearly mapped (Figures 10 and 11).

5.2. Distribution of Depositional Facies

Based on our results of depositional facies and lithological analysis, cross sections trending S-N and E-W have been constructed. It shows the distribution of facies with sandstone groups at lateral and vertical directions in the reservoir zone (Figure 14). The types and spatial distribution of distributary channels and other facies associations are also recognized in non-cored wells with the help of electro-facies of logs. From stratigraphic analysis, five sandstone groups were correlated and separated by mudstones (described in methodology part). Overall, it shows a fining upward trend in lateral and vertical directions bounded by sequence boundaries at the south (Figure 14). The direction of sedimentation is towards the north, and the upper Es3z2+3 sand group contains thick mudstone layers, while other sandstone bodies are predominantly composed of thick distributary channels (each up to 20 m) that are prograding towards the basin side (Figures 14 and 15). These deposits have good lateral continuity, up to an average 2900 m in cross section profile. Sandstones, siltstone and mudstones show a longitudinal geometry in different facies associations. It shows a variation in alternate layers of distributary and interdistributary channels with natural levee in upper and lower sandstone bodies (Figure 14). Facies associations of mouth bar contain an average thickness of 60 m in the middle intervals of Es3z4, Es3z5 and Es3z6+7 sand groups at the basin side. The average thickness of all sandstone groups is up to 150 m on the southern side, which varies up to 250 m towards the north.
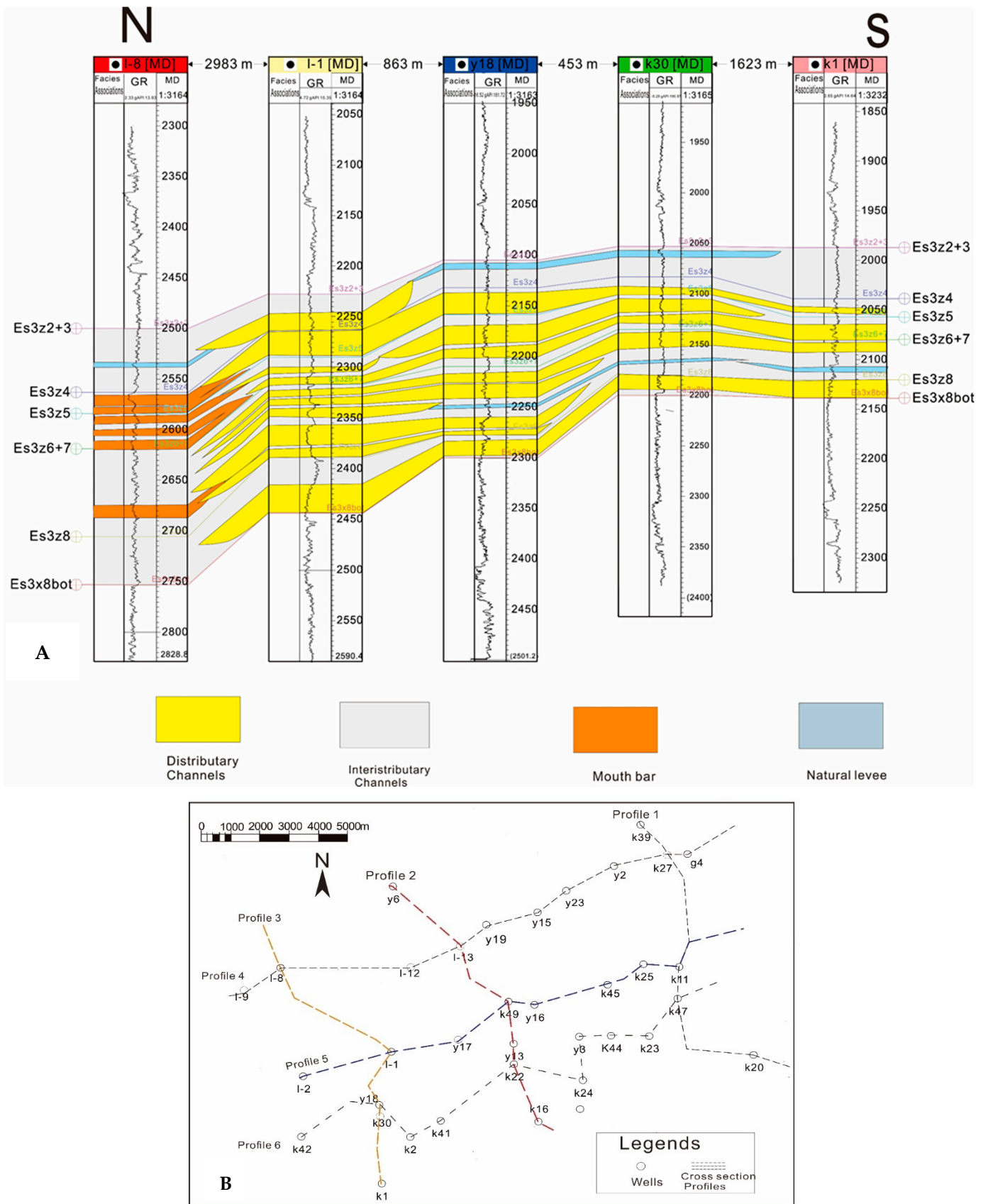
Figure 14. (**A**) Cross section profile 3 of facies associations in five sandstones group, showing facies to facies correlations from south to north. (**B**) Cross section of all profiles.
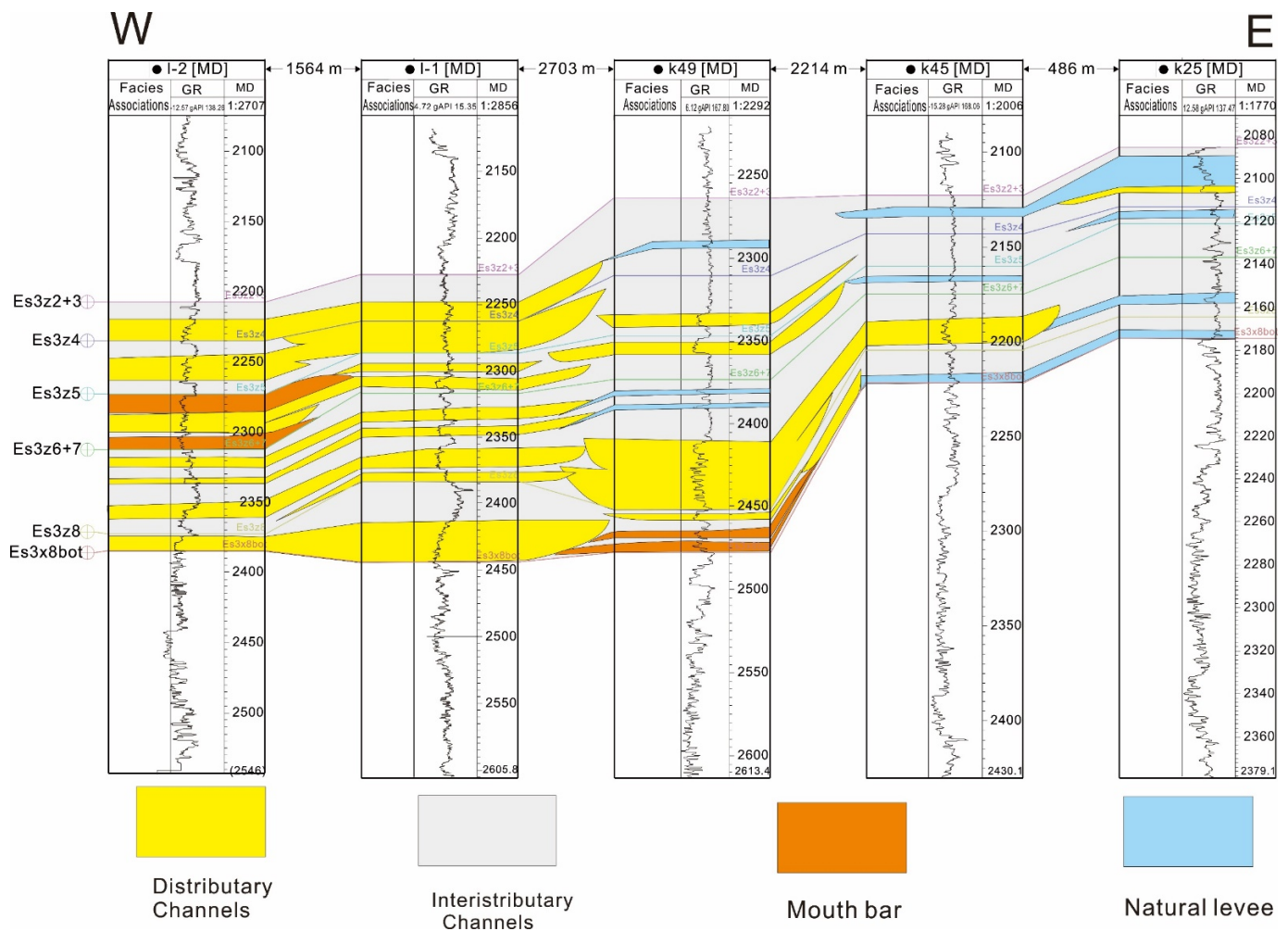
Figure 15. Cross section profile 5 of facies associations in five sandstones groups. showing facies to facies correlations from east to west direction.

In the east-west sedimentary profiles, sandstone bodies have multiple sedimentary centers on the slope belt (Figure 15). The same geometry of the finning upward sequence is found in lateral eastern and vertical directions, while on the western side, facies associations of distributary, interdistributary channels and mouth bar deposits are found in alternate layers. Facies associations in sand groups are thickened on the western side, where mudstones possess a thick pattern, along with natural levees in the eastern direction. An average thickness of 100 m was recorded in the upper, middle and the lower portion on eastern side, in which sand groups are predominantly composed of facies associations of interdistributary channels, followed by thin layers of distributary channels and natural levees. It increases up to 200 m in thickness towards the middle portion of cross section profile, in which lower units contain thick distributary channels of up to 50 m, capped by thick interdistributary channels (Figure 15). Thickness increases constantly towards the basin side in the westward direction, in which distributary channels are predominantly composed of sandstone layers, followed by facies associations of interdistributary channels and mouth bar deposits (Figure 15).

In total, five facies maps have been constructed, based on analysis of well logs, seismic and core data, which depicts a complete depositional history of facies associations in targeted sandstone group. Facies association of belt distributary channels are sourced from south-east towards north and north-west, representing a wide area along with inter-distributary channels, natural levee, sheet sand and mouth bar deposits (Figure 16A). Lithology of natural levees are associated with distributary channels and their intermediate

areas. Mouth bar has well sorted sandstones at the terminal side of the distributary channels, followed by sheet sand, ranging in thickness from 0.5 to 1 m [35] (Figures 8 and 17). The terminal side of the distributary channels show aqueous or sub-aqueous extension and represents a transitional area where the river from the delta front flows into a shallow to deep lake [41] and deposits a fine-grained sandstone (Figure 8). During the flooding periods, this area is under the influence of high-driven flow processes [32]. Mouth bars or mudstones are scoured by terminal distributary channels, both in shallow and deep lakes (Figure 16A).
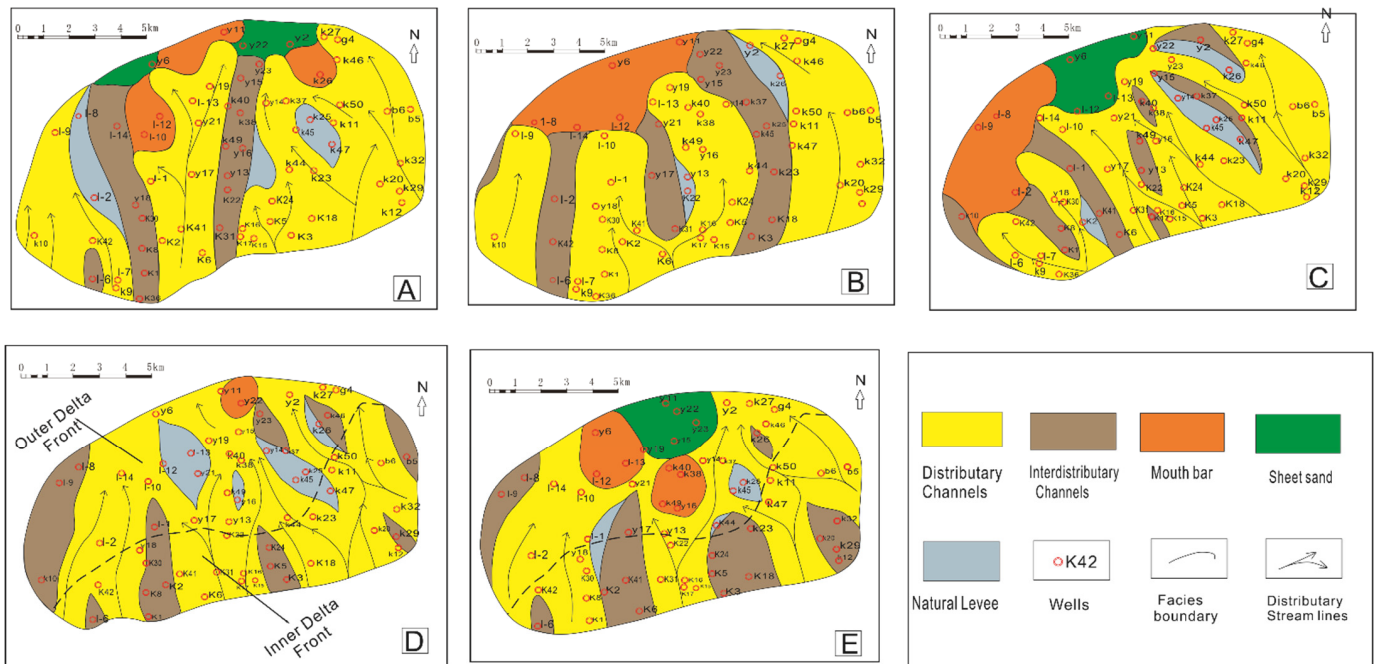
Figure 16. Distribution pattern of Facies associations in five sandstone groups (**A**) Es3z2+3, (**B**) Es3z4, (**C**) Es3z5, (**D**) Es3z6+7, (**E**) Es3z8 in the Bonan Sag. Dotted line marks a zone between outer and inner delta front facies. Interdistributary mudstone of lacustrine origin is found in wells l-8, l-9 of the lower sandstone units (Es3z6+7, Es3z8).
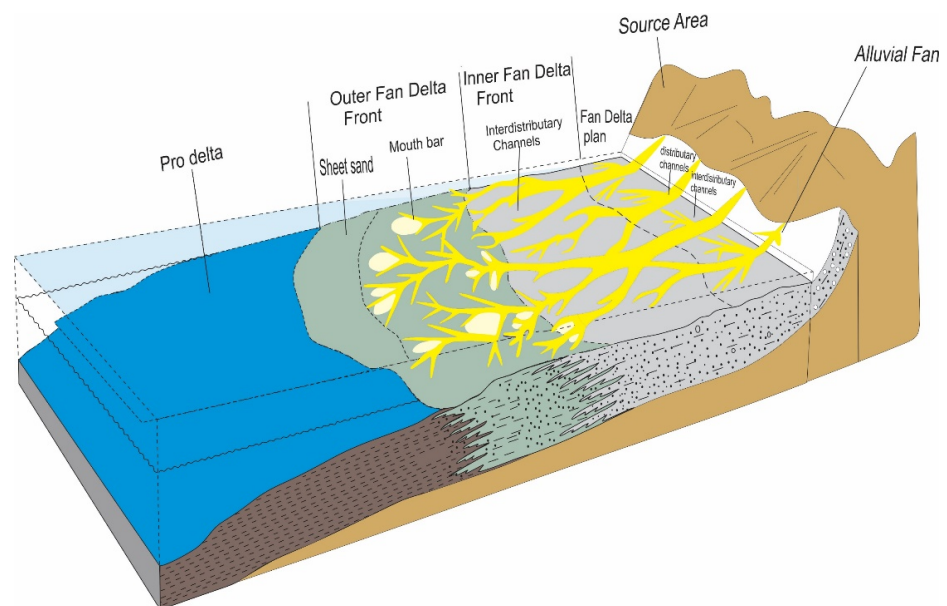

Figure 17. Generalize depositional model of coarse grain or Fan Delta.

The same sequences are seen in the second sandstone group that contains thick packages of belt distributary channels (Figure 16B). In Es3z4, facies associations of coursing upward mouth bar deposits are found at the northern side in the outer delta front. Distributary channels transport coarser sediments from the inner-delta front and the flow velocity of channels get reduced when water enters into the stagnant water of the lake. In these conditions, sediments are deposited at the mouth of the channels, initially coarser material is deposited later on medium to fine sandstone deposited in a low energy environment towards the outer-delta front (Figures 7 and 16B). Es3z4 contains fine to medium grained sandstones in facies associations of distributary channels at the middle portion of the delta front. It grades from siltstone to coarser material from the bottom to the top near the source area. Facies associations of interdistributary channels are smoothly developed from south to north, containing thick layers of gray to dark mudstones, and muddy siltstones along with sandy contents in mudstones (Figure 16B). However, a natural levee rarely occurs between distributary and interdistributary channels (Figure 16B). From the inner to outer delta front, redox and wet conditions are changed due to the influence of the shallow to deep lake (Figure 5B,C).

Sheet sands are deposited at the edge of the delta front, when water energy is reworked and deposits silt and fine sand sized particles. The wave current in a shallow lake is considered to be weakened in a river dominated delta. Therefore, sheet sand possesses the small area and sometimes it misses (Figure 16B), however, when the wave current is increased, we found that sheet sand occupied little more space. Micro normal as well as reserves faults are found in such lithologies, and these micro faults create micro fractures, which are important with regard to affecting the diagenetic property, the significance of which is revealed during the investigation of carbonate reservoirs [42]. The Es3z5 sand group contains all five facies' associations, in which distributary channels consist of conglomeratic sandstones (CSg) in the inner delta front. When water is reworked and the grained size of the channel sandstone is drastically varied from coarse to medium and fine grained towards the basin side, we found (PBSs). Conversely, mouth bar deposits are found at the north-western region in the Es3z5 adjacent to sheet sand and contain (PLS) (Figure 16C) and natural levees are widely distributed in Es3z5 and Es3z6+7 sand units.

Variegated mudstones were found in the inner delta front in the northwest direction, containing calcareous contents. It is differentiated from the mudstone in the inner delta front on the basis of color (DGM), and hence interpreted to be occurring in the outer delta front deposits in wells l-9,1-8 and l-10 (Figure 16D). In the inner delta front, we found (GM) and (GGM) deposits. The Es3z6+7 and Es3z8 sand groups are commercially very important for hydrocarbon exploration [18]. These sand groups consist of variegated sandstones, which contain the deposits of MCS, PCSS, MS, RCL, WCS in Es3z8, and RCS, CFs, BFS lithofacies in Es3z6+7 sand groups, respectively.

6. Conclusions

Sandstones of Es3z were analyzed through detailed scrutinization of cores, and interpretation of well logs and seismic data. Typical responses of well logs were calibrated with lithological associations and sedimentary structures of cores. Studies of cores and well logs show that the main lithology of reservoir units in the research area are mudstone, muddy sandstone, fine to coarse sandstone and conglomeratic sandstone along with distinguished sedimentary characteristics in five sandstone groups. Sedimentary features include cross-bedding, wedge shaped cross-bedding, parallel laminations, parallel bedding, deformed and convolute bedding.

Facies within the depositional environment of the fan delta front are interpreted in Es3z sandstone groups in the Bonan Sag of the Bohai Bay Basin, the top and bottom boundaries of which are defined regionally and calibrated with a synthetic seismogram for correlation. Facies associations are categorized on the basis of sedimentary structures, color of respective core, lithology and trend of well log response. In total, five depositional facies associations were identified in five sandstone groups, including distributary channels,

inter-distributary channels, natural levee, mouth bar and sheet sand. Mouth bar and sheet sands are missing in inner delta front deposits, while these facies are abundantly present in the outer delta front.

High gamma ray log values characterize in mudstones accumulated in inter-distributary channels that contain GM, GGM, DGM lithofacies, while distributary channels show bell and box shape on the gamma ray log, and consist of MCS, CSg, PCSs, MS, RCL, WCS, PBSs, RCS and GBS lithofacies. Funneled or coarsening upward sequences are interpreted for mouth bar deposits that have PLS, CFs and CS lithofacies. On the other hand, serrated shaped curves are observed in sheet sands, which possess the lithofacies of CBS and SSM and natural leave deposits occupiing the DFs, and serrated shaped coarsening upward siltstone deposits in the whole study area.

Based on seismic, core and well log data, five facies maps for five sandstones groups were developed to depict the depositional history of the study area. Sediments were sourced from the southeast and thicken towards the north and the northwest. The study area lies in a slope belt, and belt distributary channels covered a wide area representing the potential reservoirs, along with mouth bar deposits. Mudstones lie at the top and the bottom of sandstone reservoirs, and act as a source and seal rocks, and complete the whole petroleum system. A generalized depositional model was also developed in the study area that illustrates the distribution of facies in the outer and inner delta front. Current studies will assist future researchers to pursue reservoir modelling and simulation studies. The methodology adopted has great potential to explore the reservoirs of the fan delta front deposits in other areas.

Author Contributions: N.F.: Conceptualization, Methodology, Software, Writing—original draft preparation, Formal analysis; T.L.: Resources, Supervision, Investigation, Project administration, funding acquisition; D.F.: Formal analysis, writing review and editing, Validation; Q.A.A.: Visualization, writing review and editing. All authors have read and agreed to the published version of the manuscript.

Institutional Review Board Statement: Not applicable.

Informed Consent Statement: Not applicable.

Data Availability Statement: Not applicable.

Conflicts of Interest: The authors declare no conflict of interest.

Abbreviations

MCS	Matrix supported conglomeratic sandstone
CSg	Conglomeratic sandstone with intercalated angular gravels
PCSs	Parallel and cross bedded silty sandstone
MS	Massive sandstone
RCL	Ripple cross laminated sandstone
WCS	Wedged shape cross bedding in silty sandstone
PBSs	Parallel bedding in siltstone
RCS	Sandstone with rip up clasts
GBS	Grayish-brown sandstone
GM	Grayish mudstone
GGM	Greenish gray mudstone

DGM	Dark gray mudstone
CS	Coarsening upward sandstone
CFs	Coarsening upward fine sandstone
PLS	Parallel laminated sandstone
DFs	Deformed siltstone
CBS	Convolute bedding in siltstone
SSM	Synsedimentary faults

References

1. Hu, S.; O'Sullivan, P.B.; Raza, A.; Kohn, B.P. Thermal History and Tectonic Subsidence of the Bohai Basin, Northern China: A Cenozoic Rifted and Local Pull-Apart Basin. *Phys. Earth Planet. Inter.* **2001**, *126*, 221–235. [CrossRef]
2. Wang, Y.; Liang, C.; Sun, X. Shale Oil Reservoir Characteristics and Enrichment in the Jiyang Depression, Bohai Bay Basin, East China. *J. Earth Sci.* **2017**, *28*, 977–986. [CrossRef]
3. Feng, Y.; Liu, H.; Song, G.; Yuan, F.; Li, J.; Jiang, Z. Relationship between Decreased Pressure Gradient and Reservoir Filling Degree of Paleogene in Bonan Sag. *J. Pet. Sci. Eng.* **2019**, *180*, 615–630. [CrossRef]
4. Liu, H.; Jiang, Y.; Song, G.; Gu, G.; Hao, L.; Feng, Y. Overpressure Characteristics and Effects on Hydrocarbon Distribution in the Bonan Sag, Bohai Bay Basin, China. *J. Pet. Sci. Eng.* **2017**, *149*, 811–821. [CrossRef]
5. Yin, X.; Lu, S.; Wang, P.; Wang, Q.; Wang, W.; Yao, T. A Three-Dimensional High-Resolution Reservoir Model of the Eocene Shahejie Formation in Bohai Bay Basin, Integrating Stratigraphic Forward Modeling and Geostatistics. *Mar. Pet. Geol.* **2017**, *82*, 362–370. [CrossRef]
6. Zhang, S.; Sui, F.; Lin, H.; Liu, H.; Zhang, S.; Li, J. *Petroleum Geology and Prospective Evaluation of Pretertiary in Bohai Bay Basin*, 2nd ed.; Geological Publishing House: Beijing, China, 2008; p. 20.
7. Xiaomin, Z.; Qianghu, L.; Jiawang, G.; Yanlei, D.; Shifa, Z.; Mingxuan, T.; Yong, Y. Reconstruction of sediment-dispersal patterns using seismic sedimentology in the southeastern Zhanhua Sag, Bohai Bay Basin, China. *J. Pet. Sci. Eng.* **2019**, *182*, 106335. [CrossRef]
8. Liu, Q.; Zhu, Q.; Zhu, H.; Liu, k.; Tan, M.; Chen, H. Three-dimensional forward stratigraphic modelling of the gravel-to mud-rich fan-delta in the slope system of Zhanhua Sag, Bohai Bay Basin, China. *Mar. Pet. Geol.* **2017**, *70*, 18–30. [CrossRef]
9. Lai, J.; Wang, G.; Fan, Z.; Chen, J.; Wang, S.; Fan, X. Sedimentary Characterization of a Braided Delta Using Well Logs: The Upper Triassic Xujiahe Formation in Central Sichuan Basin, China. *J. Pet. Sci. Eng.* **2017**, *154*, 172–193. [CrossRef]
10. Tong, K.J.; Zhao, C.M.; Lu, Z.B.; Zhang, Y.C.; Zheng, H.; Xu, S.N.; Wang, J.L.; Pan, L.L. Reservoir evaluation and fracture chracterization of the metamorphic buried hill reservoir in Bohai Bay Basin. *Pet. Explor. Dev.* **2012**, *39*, 62–69. [CrossRef]
11. Huo, G.; Qian, X.; Song, X. The Origin of the Bohai Bay Basin. *Acta Sci. Nat. Univ. Pekin.* **1998**, *34*, 503–509.
12. Allen, M.B.; Macdonald, D.I.M.; Xun, Z.; Vincent, S.J.; Brouet-Menzies, C. Early Cenozoic Two-Phase Extension and Late Cenozoic Thermal Subsidence and Inversion of the Bohai Basin, Northern China. *Mar. Pet. Geol.* **1997**, *14*, 951–972. [CrossRef]
13. Qi, J.; Yang, Q. Cenozoic Structural Deformation and Dynamic Processes of the Bohai Bay Basin Province, China. *Mar. Pet. Geol.* **2010**, *27*, 757–771. [CrossRef]
14. Qi, J. Two Tectonic Systems in the Cenozoic Bohai Bay Basin and Their Genetic Interpretation. *Chin. Geol.* **2004**, *31*, 15–22.
15. Zhao, F.; Jiang, S.; Li, S.; Zhang, H.; Wang, G.; Lei, J.; Gao, S. Cenozoic Tectonic Migration in the Bohai Bay Basin, East China. *Geol. J.* **2016**, *51*, 188–202. [CrossRef]
16. Dong, C. High Revolution Sequence Stratigraphy in Third Member of Shahejie Formation of the Lower Tertiary in Bonan Sag. *J. Univ. Pet. China Ed. Nat. Sci.* **2002**, *26*, 11–14.
17. Wang, M.; Wilkins, R.W.T.; Song, G.; Zhang, L.; Xu, X.; Li, Z.; Chen, G. Geochemical and Geological Characteristics of the Es3L Lacustrine Shale in the Bonan Sag, Bohai Bay Basin, China. *Int. J. Coal Geol.* **2015**, *138*, 16–29. [CrossRef]
18. Fawad, N.; Liu, T.; Fan, D.; Qazi, M.A. Sequence stratigraphic division and correlation of third middle member of Eocene Shahejie formation in the Bonan Sag, Bohai Bay Basin, China. In Proceedings of the 5th International Conference of Palaeogeography, Yangzte Univertsity, Wuhan, China, 12–15 May 2022.
19. Nazeer, A.; Abbasi, A.S.; Sarfraz, S.H. Sedimentary facies interpretation of Gamma Ray (GR) log as basic well logs in Central and Lower Indus Basin of Pakistan. *Geod. Geodyn.* **2016**, *10*, 1–12. [CrossRef]
20. Selley, R.C. *Concepts and Methods of Subsurface Facies Analysis*; American Association of Petroleum Geologists: Tulsa, OK, USA, 1978; pp. 9–82.
21. Nichols. *Sedimentology and Stratigraphy*, 2nd ed.; John Wiley & sons Ltd.: Chichester, UK, 2009; pp. 1–411.
22. Guo, L.; Jia, C.; Konhauser, K.O. Depositional system and hydrocarbon accumulation in Gubei slope zone, Zhanhua Depression, Bohai Bay Basin, eastern China. *Energy Explor. Exploit.* **2016**, *34*, 810–827. [CrossRef]
23. Jiang, S.; Henriksen, S.; Wang, H.; Lu, Y.; Ren, J.; Cai, D.; Feng, Y.; Weimer, P.J. Sequence-stratigraphic architectures and sand-body distribution in Cenozoic rifted lacustrine basins, east China. *Am. Assoc. Pet. Geol. Bull.* **2013**, *97*, 1447–1475. [CrossRef]
24. Lu, S.; Liu, W.; Wang, M.; Zhang, L.; Wang, Z.; Chen, G.; Xiao, D.; Li, Z.; Hu, H.T. Lacustrine shale oil resource potential of Es3L Sub-Member of Bonan Sag, Bohai Bay Basin, Eastern China. *J. Earth Sci.* **2017**, *28*, 996–1005. [CrossRef]
25. Hu, L. Pressure characteristics and formation mechanisms of Paleogene in Bonan sag, Zhanhua depression. *J. China Univ. Pet.* **2013**, *37*, 46–51.

26. Yuan, J.; Yu, G.; Song, M.; Zhong, J.; Dong, D.; Wang, W.; Liu, Y.; Ma, L. Depositional characteristics and reservoir potential of Paleogene sediment gravity flow deposits on a faulted slope of the Zhanhua Sag, Bohai Bay Basin, China. *J. Asian Earth. Sci.* **2019**, *177*, 89–106. [CrossRef]

27. Zhu, X.; Zeng, H.; Li, S.; Dong, Y.; Zhu, S.; Zhao, D.; Huang, W. Sedimentary characteristics and seismic geomorphologic responses of a shallow-water delta in the Qingshankou Formation from the Songliao Basin, China. *Mar. Petrol. Geol.* **2017**, *79*, 131–148. [CrossRef]

28. Marriott, S.B.; Wright, V.P. Mudrock deposition in an ancient dryland system: Moor Cliffs Formation, Lower Old Red Sandstone, southwest Wales. *UK Geol. J.* **2004**, *39*, 277–298. [CrossRef]

29. Li, Z.; Zhi, D.B.; Lu, X.D.; Dong, S.Z.; Shu, W.M.; Jian, S.; Jia, H.Z.; Ze, C.W. Sedimentary characteristics and pattern of distributary channels in shallow water deltaic red bed succession: A case from the Late Cretaceous Yaojia formation, southern Songliao Basin, NE China. *J. Pet. Sci. Eng.* **2018**, *171*, 1171–1190.

30. Li, Y.; Shao, L.; Eriksson, K.A.; Tong, X.; Gao, C.; Chen, Z. Linked Sequence Stratigraphy and Tectonics in the Sichuan Continental Foreland Basin, Upper Triassic Xujiahe Formation, Southwest China. *J. Asian Earth Sci.* **2014**, *88*, 116–136. [CrossRef]

31. Zhou, Y.; Ji, Y.; Pigott, J.D.; Meng, Q.; Wan, L. Tectono-stratigraphy of Lower Cretaceous Tanan sub-basin, Tamtsag Basin, Mongolia: Sequence architecture, depositional systems and controls on sediment infill. *Mar. Pet. Geol.* **2014**, *49*, 176–202. [CrossRef]

32. Van, D.K.D.A.; Flaig, P.P.; Hasiotis, S.T. Paleoenvironmental Reconstruction of A Late Cretaceous, Muddy, River-Dominated Polar Deltaic System: Schrader Bluff Prince Creek Formation Transition, Shivugak Bluffs, North Slope of Alaska. *USA J. Sediment. Res.* **2015**, *85*, 903–936.

33. Dong, W.; Lin, C.; Eriksson, K.; Zhou, X.; Liu, J.; Teng, Y. Depositional Systems and Sequence Architecture of the Oligocene Dongying Formation, Liaozhong Depression, Bohai Bay Basin, Northeast China. *Am. Assoc. Pet. Geol. Bull.* **2011**, *95*, 1475–1493. [CrossRef]

34. Li, S.; Ma, Y.Z.; Yu, X.; Li, S. Reservoir potential of deep water lacustrine delta-front sandstones in upper Triassic yangchang formation, Western Ordos Basin, China. *J. Pet. Geol.* **2017**, *40*, 105–118. [CrossRef]

35. Martini, I.; Sandrelli, F. Facies analysis of a Pliocene river-dominated deltaic succession (Siena Basin, Italy): Implications for the formation and infilling of terminal distributary channels. *Sedimentology* **2015**, *62*, 234–265. [CrossRef]

36. Boggs. *Petrology of Sedimentary Rocks*, 2nd ed.; Cambridge University Press: London, UK, 2009; pp. 1–167.

37. Tanner, L.H.; Lucas, S.G. Deposition and deformation of fluvial–lacustrine sediments of the Upper Triassic–Lower Jurassic Whitmore Point Member, Moenave Formation, northern Arizona. *Sediment. Geol.* **2010**, *223*, 180–191. [CrossRef]

38. Ming-zhen, W. The Discovery and Geological Preliminary Investigation of A Slump-Slip Soft-Sediment Deformation Multilayer Complex Structure in Neoproterozoic Strata in Shouxian County, Anhui Province. *Acta Geosci. Sin.* **2012**, *1*, 49–56.

39. Shanmugam, G. Modern Internal Waves and Internal Tides along Oceanic Pycnoclines: Challenges and Implications for Ancient Deep-Marine Baroclinic Sands. Am. *Assoc. Pet. Geol. Bull.* **2013**, *97*, 799–843. [CrossRef]

40. Luo, S.; He, S.; Jin, Q.; Yang, R.; Zhang, J. Overpressure System Classification and Structure Characteristic in Bonan Sag. *J. Jilin Univ. Earth Sci. Ed.* **2015**, *45*, 37–51. [CrossRef]

41. Olariu, C.; Steel, R.J.; Petter, A.L. Delta-front hyperpycnal bed geometry and implications for reservoir modeling: Cretaceous Panther Tongue delta, Book Cliffs, Utah. *Am. Assoc. Petrol. Geol. Bull.* **2010**, *94*, 819–845. [CrossRef]

42. Maniscalco, R.; Fazio, E.; Punturo, R.; Cirrincione, R.; Di Stefano, A.; Distefano, S.; Forzese, M.; Lanzafame, G.; Leonardi, G.S.; Montalbano, S.; et al. The Porosity in Heterogeneous Carbonate Reservoir Rocks: Tectonic versus Diagenetic Imprint—A Multi-Scale Study from the Hyblean Plateau (SE Sicily, Italy). *Geosciences* **2022**, *12*, 149. [CrossRef]